

Location and Scale-Invariant Power Transformations for Transforming Data to Normality

Alex Zwanenburg^{1,2*} and Steffen Löck^{2,3,4}

^{1*} National Center for Tumor Diseases (NCT), NCT/UCC Dresden , a partnership between DKFZ, Faculty of Medicine and University Hospital Carl Gustav Carus, TUD Dresden University of Technology, and Helmholtz-Zentrum Dresden-Rossendorf (HZDR), Fetscherstraße 74/PF 64, Dresden, 01307, Germany .

² OncoRay - National Center for Radiation Research in Oncology Faculty of Medicine and University Hospital Carl Gustav Carus, TUD Dresden University of Technology, Helmholtz-Zentrum Dresden-Rossendorf, Fetscherstraße 74/PF 41, Dresden, 01307, Germany .

³ Department of Radiotherapy and Radiation Oncology, Faculty of Medicine and University Hospital Carl Gustav Carus, TUD Dresden University of Technology, Fetscherstraße 74/PF 50, Dresden, 01307, Germany .

⁴ German Cancer Consortium (DKTK), Partner Site Dresden, German Cancer Research Center (DKFZ), Im Neuenheimer Feld 280, Heidelberg, 69192, Germany .

*Corresponding author(s). E-mail(s):
alexander.zwanenburg@nct-dresden.de;
Contributing authors: steffen.loeck@oncoray.de;

Abstract

Power transformations are used to stabilize variance and achieve normality of features, especially in methods assuming normal distributions such as ANOVA and linear discriminant analysis. However, the commonly used Box-Cox and Yeo-Johnson power transformation methods are sensitive to the location, scale, and presence of outliers in the data. Here we present location- and scale-invariant Box-Cox and Yeo-Johnson transformations to mitigate these issues. We derive

maximum likelihood estimation criteria for optimizing transformation parameters and propose robust adaptations that reduce the influence of outliers. We also introduce an empirical test for assessing central normality of transformed features. In simulations and real-world datasets, robust location- and scale-invariant transformations outperform conventional variants, resulting in better transformations to central normality. In a machine learning experiment with 231 datasets with numerical features, integrating robust location- and scale-invariant power transformations into an automated data processing and machine learning pipeline did not result in a meaningful improvement or detriment to model performance compared to conventional variants. In conclusion, robust location- and scale-invariant power transformations can replace conventional variants.

Keywords: Data preprocessing, Feature transformation, Outliers, Power transformation

1 Introduction

Many statistical and some machine learning methods assume normality of the underlying data, e.g. analysis of variance and linear discriminant analysis. However, numerical features in datasets may strongly deviate from normal distributions, e.g. by being skewed. Power transformations aim to stabilise variance and improve normality of such features (Bartlett, 1947; Tukey, 1957). The two most commonly used transformations are that of Box and Cox (1964) and Yeo and Johnson (2000).

The Box-Cox transformation is defined as:

Definition (Box-Cox power transformation). *Let $\mathbf{X} = \{x_1, x_2, \dots, x_n | x_i > 0\}$ be a finite sequence of length $n > 0$. Let $\lambda \in \mathcal{R}$ be a transformation parameter. Then the Box-Cox power transformation of element x_i is defined as:*

$$\phi_{BC}^\lambda(x_i) = \begin{cases} (x_i^\lambda - 1) / \lambda & \text{if } \lambda \neq 0 \\ \log(x_i) & \text{if } \lambda = 0 \end{cases} \quad (1)$$

One limitation of the Box-Cox transformation is that it is only defined for $x_i > 0$. In contrast, the Yeo-Johnson transformation under the transformation parameter λ is defined for any $x_i \in \mathbb{R}$, as follows:

Definition (Yeo-Johnson power transformation). *Let $\mathbf{X} = \{x_1, x_2, \dots, x_n | x_i \in \mathbb{R}\}$ be a finite sequence of length $n > 0$. Let $\lambda \in \mathcal{R}$ be a transformation parameter.*

$$\phi_{YJ}^\lambda(x_i) = \begin{cases} ((1 + x_i)^\lambda - 1) / \lambda & \text{if } \lambda \neq 0 \text{ and } x_i \geq 0 \\ \log(1 + x_i) & \text{if } \lambda = 0 \text{ and } x_i \geq 0 \\ -((1 - x_i)^{2-\lambda} - 1) / (2 - \lambda) & \text{if } \lambda \neq 2 \text{ and } x_i < 0 \\ -\log(1 - x_i) & \text{if } \lambda = 2 \text{ and } x_i < 0 \end{cases} \quad (2)$$

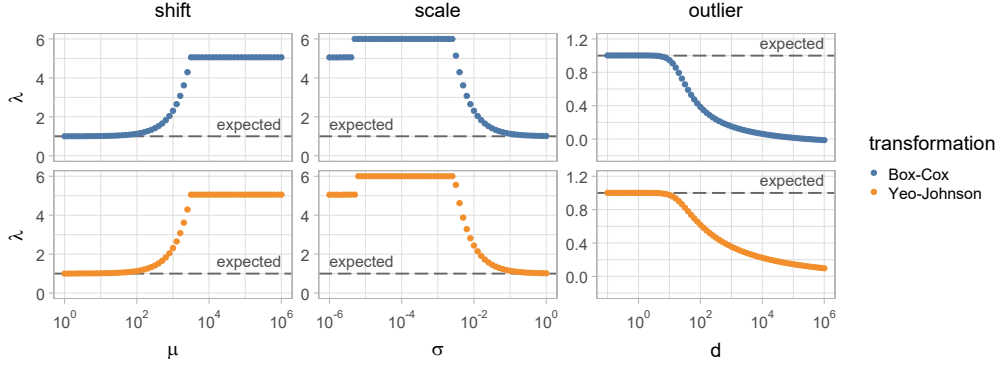


Fig. 1 Effect of location, scale and outliers on estimation of the Box-Cox and Yeo-Johnson transformation parameter λ . 10000 samples were drawn from a normal distribution: $\mathcal{N}(\mu, 1)$ for the *shift* dataset, $\mathcal{N}(10, \sigma)$ for the *scale* dataset and $\mathcal{N}(0, 1)$ for the *outlier* dataset. Additionally, an outlier with value d was added to the outlier dataset. Since samples are drawn from a normal distribution, a transformation parameter of $\lambda = 1$ is expected. However, a large shift in location, a scale that is small compared to the location, or presence of large outliers lead to incorrectly estimated transformation parameter values.

The λ -parameter is typically optimised using maximum likelihood estimation under the assumption that the transformed feature is normally distributed. As noted by Raymaekers and Rousseeuw, this approach is sensitive to outliers, and robust versions of Box-Cox and Yeo-Johnson transformations were devised (Raymaekers & Rousseeuw, 2024).

Applying a power transformation does not guarantee that transformed features are normally distributed. Depending on location and scale of a feature and the presence of outliers, power transformations may decrease normality, as shown in Figure 1. If normality of the transformed feature is not checked, e.g. in automated power transformation in machine learning workflows, several issues may arise. For example, statistical tests such as ANOVA may produce incorrect results due to violation of the normality assumption. Likewise, machine learning methods that assume normality of input features may suffer a decrease in performance. Moreover, large negative or positive λ -parameters may lead to numeric issues in any subsequent computations.

Statistical tests for normality, such as the Shapiro-Wilk test (Shapiro & Wilk, 1965), could be automatically applied to transformed features. However, given sufficiently large sample sizes such tests can detect trivial deviations from normality, and may lead to rejection of sufficiently good power transformations.

To address these issues, we make the following contributions:

- We devise location- and scale-invariant versions of the Box-Cox and Yeo-Johnson transformation, including versions robust to outliers.
- We derive the maximum likelihood criterion for location- and scale-invariant Box-Cox and Yeo-Johnson transformations to allow for optimising transformation parameters.
- We define an empirical central normality test for detecting cases where power transformations fail to yield an approximately normally distributed transformed feature.

- We assess the effect of power transformations on the performance of machine learning models.

2 Theory

In this section, we will first introduce location- and scale-invariant versions of the Box-Cox and Yeo-Johnson transformations. Subsequently, we define weighted location- and scale-invariant transformations and weighting methods for robust transformations. We then define the quantile function for asymmetric generalised normal distributions to enable random sampling. Finally, we define the overall framework for the empirical central normality test.

First, we define a (numeric) feature. Throughout this work, whenever reference is made to a feature, a numeric feature is meant unless noted otherwise.

Definition (Numeric feature). *A numeric feature is a finite sequence $\mathbf{X} = \{x_1, x_2, \dots, x_n | x_i \in \mathbb{R}\}$ of length n .*

2.1 Location- and scale-invariant power transformation

Box and Cox (1964) originally included a shift parameter in their transformation, but for their formal analysis set it to 0, whereas Yeo and Johnson (2000) did not include a shift or scale parameter. Here, Box-Cox and Yeo-Johnson transformations are modified by introducing shift parameter x_0 and scale parameter s into equations 1 and 2. The location- and scale-invariant Box-Cox transformation of a feature value x_i of feature \mathbf{X} under transformation parameter λ , shift parameter x_0 and scale parameter s is then defined as:

Definition (Location- and scale- invariant Box-Cox power transformation). *Let $\lambda \in \mathbb{R}$ be a transformation parameter. Let $x_0 \in \mathbb{R}$ and $s > 0$ be location and scale parameters. Let $\mathbf{X} = \{x_1, x_2, \dots, x_n | x_i - x_0 > 0\}$ be a finite sequence of length $n > 0$.*

Then the location- and scale-invariant Box-Cox power transformation of element x_i is defined as:

$$\phi_{BC}^{\lambda, x_0, s}(x_i) = \begin{cases} \left(\left(\frac{x_i - x_0}{s} \right)^\lambda - 1 \right) / \lambda & \text{if } \lambda \neq 0 \\ \log \left[\frac{x_i - x_0}{s} \right] & \text{if } \lambda = 0 \end{cases} \quad (3)$$

Likewise, the location- and scale-invariant Yeo-Johnson transformation of a feature value x_i under transformation parameter λ , shift parameter x_0 and scale parameter s is defined as:

Definition (Location- and scale- invariant Yeo-Johnson power transformation). *Let $\lambda \in \mathbb{R}$ be a transformation parameter. Let $x_0 \in \mathbb{R}$ and $s > 0$ be location and scale parameters. Let $\mathbf{X} = \{x_1, x_2, \dots, x_n | x_i \in \mathbb{R}\}$ be a finite sequence of length $n > 0$.*

Then the location- and scale-invariant Yeo-Johnson power transformation of element x_i is defined as:

$$\phi_{YJ}^{\lambda, x_0, s}(x_i) = \begin{cases} \left(\left(1 + \frac{x_i - x_0}{s} \right)^\lambda - 1 \right) / \lambda & \text{if } \lambda \neq 0 \text{ and } x_i - x_0 \geq 0 \\ \log \left[1 + \frac{x_i - x_0}{s} \right] & \text{if } \lambda = 0 \text{ and } x_i - x_0 \geq 0 \\ - \left(\left(1 - \frac{x_i - x_0}{s} \right)^{2-\lambda} - 1 \right) / (2 - \lambda) & \text{if } \lambda \neq 2 \text{ and } x_i - x_0 < 0 \\ - \log \left[1 - \frac{x_i - x_0}{s} \right] & \text{if } \lambda = 2 \text{ and } x_i - x_0 < 0 \end{cases} \quad (4)$$

For both invariant transformations, λ , x_0 and s parameters can be obtained by maximising the log-likelihood function, i.e. using maximum likelihood estimation (MLE). A full derivation of the log-likelihood function for both transformations is shown in [Appendix A](#). The location- and scale-invariant Box-Cox log-likelihood function is:

Definition (Log-likelihood function of the location- and scale- invariant Box-Cox power transformation). *Let \mathbf{X} , λ , x_0 , and s be defined as earlier (Eqn. 3). Let μ and σ^2 be the mean and variance of the transformed sequence $\phi_{BC}^{\lambda, x_0, s}(\mathbf{X})$, respectively.*

Then the log-likelihood function of the location- and scale- invariant Box-Cox power transformation is defined as:

$$\begin{aligned} \mathcal{L}_{BC}^{\lambda, x_0, s} = & -\frac{n}{2} \log [2\pi\sigma^2] - \frac{1}{2\sigma^2} \sum_{i=1}^n \left(\phi_{BC}^{\lambda, x_0, s}(x_i) - \mu \right)^2 \\ & - n\lambda \log s + (\lambda - 1) \sum_{i=1}^n \log [x_i - x_0] \end{aligned} \quad (5)$$

Similarly, the location- and scale-invariant Yeo-Johnson log-likelihood function is:

Definition (Log-likelihood function of the location- and scale- invariant Yeo-Johnson power transformation). *Let \mathbf{X} , λ , x_0 , and s be defined as earlier (Eqn. 4). Let μ and σ^2 be the mean and variance of the transformed sequence $\phi_{YJ}^{\lambda, x_0, s}(\mathbf{X})$, respectively.*

Then the log-likelihood function of the location- and scale- invariant Yeo-Johnson power transformation is defined as:

$$\begin{aligned} \mathcal{L}_{YJ}^{\lambda, x_0, s} = & -\frac{n}{2} \log [2\pi\sigma^2] - \frac{1}{2\sigma^2} \sum_{i=1}^n \left(\phi_{YJ}^{\lambda, x_0, s}(x_i) - \mu \right)^2 \\ & - n \log s + (\lambda - 1) \sum_{i=1}^n \operatorname{sgn}(x_i - x_0) \log \left[1 + \frac{|x_i - x_0|}{s} \right] \end{aligned} \quad (6)$$

2.2 Robust location- and scale-invariant power transformations

Real-world data may contain outliers, to which maximum likelihood estimation can be sensitive. Their presence may lead to poor transformations to normality, as shown in Figure 1. As indicated by [Raymaekers and Rousseeuw \(2024\)](#), the general aim of power transformations should be to transform non-outlier data to normality, i.e. achieve *central normality*. To achieve this, they devised an iterative procedure to find a robust estimate of the transformation parameter λ . Briefly, this process requires identifying

outliers in the data and weighting such instances during the optimisation process. Raymaekers and Rousseeuw (2024) achieve this through weighted maximum likelihood estimation. However, because this procedure iteratively estimates and updates λ , it can not be used here to simultaneously estimate λ , x_0 and s for location- and scale-invariant power transformations. Nonetheless, as a procedure, weighted MLE can be used for estimating the transformation, shift and scale parameters.

Here, weighted maximum likelihood estimation is based on equations 5 and 6. Compared to Raymaekers and Rousseeuw (2024), these log-likelihood functions include additional terms to accommodate estimation of x_0 and s . The weighted location- and scale-invariant Box-Cox log-likelihood function is:

Definition (Weighted log-likelihood function of the location- and scale- invariant Box-Cox power transformation). *Let \mathbf{X} , λ , x_0 , and s be defined as earlier (Eqn. 3). Let $w_i \geq 0$ be the weight corresponding to each element of \mathbf{X} . Let μ_w be the weighted mean of the Box-Cox transformed sequence:*

$$\mu_w = \frac{\sum_{i=1}^n w_i \phi_{BC}^{\lambda, x_0, s}(x_i)}{\sum_{i=1}^n w_i}$$

Let σ_w^2 be the weighted variance of the Box-Cox transformed sequence:

$$\sigma_w^2 = \frac{\sum_{i=1}^n w_i (\phi_{BC}^{\lambda, x_0, s}(x_i) - \mu_w)^2}{\sum_{i=1}^n w_i}$$

Then, the weighted log-likelihood function of the location- and scale- invariant Box-Cox power transformation is:

$$\begin{aligned} \mathcal{L}_{rBC}^{\lambda, x_0, s} = & -\frac{1}{2} \left(\sum_{i=1}^n w_i \right) \log [2\pi\sigma_w^2] - \frac{1}{2\sigma_w^2} \sum_{i=1}^n w_i (\phi_{BC}^{\lambda, x_0, s}(x_i) - \mu_w)^2 \\ & - \lambda \left(\sum_{i=1}^n w_i \right) \log s + (\lambda - 1) \sum_{i=1}^n w_i \log [x_i - x_0] \end{aligned} \quad (7)$$

Analogously, the weighted location- and scale-invariant Yeo-Johnson log-likelihood function is:

Definition (Weighted log-likelihood function of the location- and scale- invariant Yeo-Johnson power transformation). *Let \mathbf{X} , λ , x_0 , and s be defined as earlier (Eqn. 4). Let $w_i \geq 0$ be the weight corresponding to each element of \mathbf{X} . Let μ_w be the weighted mean of the Yeo-Johnson transformed sequence:*

$$\mu_w = \frac{\sum_{i=1}^n w_i \phi_{YJ}^{\lambda, x_0, s}(x_i)}{\sum_{i=1}^n w_i}$$

Let σ_w^2 be the weighted variance of the Yeo-Johnson transformed sequence:

$$\sigma_w^2 = \frac{\sum_{i=1}^n w_i (\phi_{YJ}^{\lambda, x_0, s}(x_i) - \mu_w)^2}{\sum_{i=1}^n w_i}$$

Then, the weighted log-likelihood function of the location- and scale- invariant Yeo-Johnson power transformation is:

$$\begin{aligned} \mathcal{L}_{rYJ}^{\lambda, x_0, s} = & -\frac{1}{2} \left(\sum_{i=1}^n w_i \right) \log [2\pi\sigma_w^2] - \frac{1}{2\sigma_w^2} \sum_{i=1}^n w_i \left(\phi_{YJ}^{\lambda, x_0, s}(x_i) - \mu_w \right)^2 \\ & - \left(\sum_{i=1}^n w_i \right) \log s + (\lambda - 1) \sum_{i=1}^n w_i \operatorname{sgn}(x_i - x_0) \log \left[1 + \frac{|x_i - x_0|}{s} \right] \end{aligned} \quad (8)$$

The weights w_i in equations 7 and 8 can be set using several weighting functions. Using \dot{x}_i as an argument that will be defined later, we investigate three weighting functions:

- A step function, with $\delta_1 \geq 0$ as threshold parameter:

$$w_i = \begin{cases} 1 & \text{if } |\dot{x}_i| \leq \delta_1 \\ 0 & \text{if } |\dot{x}_i| > \delta_1 \end{cases}$$

- A triangle function (or generalised Huber weight), with $\delta_1 \geq 0$ and $\delta_2 \geq \delta_1$ as threshold parameters:

$$w_i = \begin{cases} 1 & \text{if } |\dot{x}_i| < \delta_1 \\ 1 - \frac{|\dot{x}_i| - \delta_1}{\delta_2 - \delta_1} & \text{if } \delta_1 \leq |\dot{x}_i| \leq \delta_2 \\ 0 & \text{if } |\dot{x}_i| > \delta_2 \end{cases}$$

- A tapered cosine function (Tukey, 1967), with $\delta_1 \geq 0$ and $\delta_2 \geq \delta_1$ as threshold parameters:

$$w_i = \begin{cases} 1 & \text{if } |\dot{x}_i| < \delta_1 \\ 0.5 + 0.5 \cos \left(\pi \frac{|\dot{x}_i| - \delta_1}{\delta_2 - \delta_1} \right) & \text{if } \delta_1 \leq |\dot{x}_i| \leq \delta_2 \\ 0 & \text{if } |\dot{x}_i| > \delta_2 \end{cases}$$

All weighting functions share the characteristic that for $|\dot{x}_i| < \delta_1$, instances are fully weighted, i.e. when $\delta_1 > 0$ the weighting functions are symmetric window functions with a flat top. The triangle and tapered cosine functions then gradually down-weight instances with $\delta_1 \leq |\dot{x}_i| \leq \delta_2$, and assign no weight to instances $|\dot{x}_i| > \delta_2$. Examples of these weighting function are shown in Figure 2.

Each weighting function has an argument \dot{x} that is related to the (transformed) feature in one of several ways:

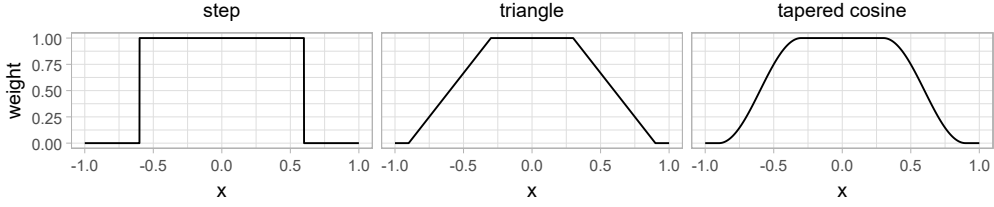


Fig. 2 Weighting functions investigated in this study to make power transformations more robust against outliers. In this example, the step function was parameterised with $\delta_1 = 0.60$. The triangle and tapered cosine functions were both parameterised with $\delta_1 = 0.30$ and $\delta_2 = 0.90$.

- The weighting function uses empirical probabilities of the distribution of the original feature \mathbf{X} . After sorting \mathbf{X} in ascending order, probabilities are determined as $p_i = \frac{i-1/3}{n+1/3}$, with $i = 1, 2, \dots, n$, with n the number of instances of feature \mathbf{X} . Then $\dot{x}_i = p_i^* = 2(p_i - 0.5)$, so that argument is zero-centered.
- The weighting function uses the z-score of the transformed feature $\phi^{\lambda, x_0, s}(\mathbf{X})$. After Raymaekers and Rousseeuw (2024), $z_i = \frac{\phi^{\lambda, x_0, s}(x_i) - \mu_M}{\sigma_M}$. Here, μ_M and σ_M are robust Huber M-estimates of location and scale of the transformed feature $\phi^{\lambda, x_0, s}(\mathbf{X})$ (Huber, 1981). Then $\dot{x}_i = z_i$.
- After sorting \mathbf{X} in ascending order, the weighting function uses the residual error between the z-score of the transformed feature $\phi^{\lambda, x_0, s}(\mathbf{X})$ and the theoretical z-score from a standard normal distribution: $r_i = |(\phi^{\lambda, x_0, s}(x_i) - \mu_M) / \sigma_M - F_N^{-1}(p_i)|$, with μ_M , σ_M and p_i as defined above. Then $\dot{x}_i = r_i$.

2.3 Asymmetric generalised normal distributions

Modifications intended to make power transformations invariant to location and scale of a feature and methods to improve their robustness against outliers need to be assessed using data drawn from a range of different distributions. Since the power transformations are intended for use with unimodal distributions, the generalised normal distribution (Nadarajah, 2005; Subbotin, 1923) is a suitable option for simulating realistic feature distributions. This distribution has the following probability density function f_β for a value $x \in \mathbb{R}$:

Definition (Standard generalised normal distribution probability density function). Let $x \in \mathcal{R}$. Let $\beta > 0$ be a shape parameter. Let Γ be the gamma function.

Then the standard generalised normal distribution probability density function, without scale and location parameters, is:

$$f_\beta(x) = \frac{\beta}{2\Gamma(1/\beta)} e^{-|x|^\beta} \quad (9)$$

For $\beta = 1$, the probability density function describes a Laplace distribution. A normal distribution is found for $\beta = 2$, and for large β , the distribution approaches a uniform distribution.

Realistic feature distributions may be skewed. Gijbels et al. describe a recipe for introducing skewness into the otherwise symmetric generalised normal distribution

(Gijbels, Karim, & Verhasselt, 2019), leading to the following probability density function:

Definition (Asymmetric generalised normal distribution probability density function). Let $\alpha \in (0, 1)$ be a skewness parameter. Let $\mu \in \mathbb{R}$ be a location parameter. Let $\sigma > 0$ be a shape parameter.

Then the probability density function of the asymmetric generalised normal distribution is:

$$f_\alpha(x; \mu, \sigma, \beta) = \frac{2\alpha(1-\alpha)}{\sigma} \begin{cases} f_\beta\left((1-\alpha)\frac{|x-\mu|}{\sigma}\right) & , x \leq \mu \\ f_\beta\left(\alpha\frac{|x-\mu|}{\sigma}\right) & , x > \mu \end{cases} \quad (10)$$

$\alpha > 0.5$ creates a distribution with a negative skew, i.e. a left-skewed distribution. A right-skewed distribution is created for $\alpha < 0.5$. f_α thus describes the probability density function of an asymmetric generalised normal distribution, which we will refer to here and parametrise as $\mathcal{AGN}(\mu, \sigma, \alpha, \beta)$.

We require a quantile function (or an approximation thereof) to draw random values from an asymmetric generalised normal distribution using inverse transform sampling. Gijbels et al. derived the quantile function $F_\alpha^{-1}(p)$, which incorporates the quantile function of the symmetric generalised normal distribution derived by Griffin (Griffin, 2018):

Definition (Asymmetric generalised normal distribution quantile function). Let $p \in [0, 1]$ be a probability. Let F_Γ^{-1} is the quantile function of the gamma distribution with shape $1/\beta$, which can be numerically approximated. Let F_β^{-1} be the quantile function of the generalised normal distribution:

$$F_\beta^{-1}(p) = \text{sgn}(p - 0.5) F_\Gamma^{-1}(2|p - 0.5|; 1/\beta) \quad (11)$$

Then the quantile function of the asymmetric generalised normal distribution is:

$$F_\alpha^{-1}(p; \mu, \sigma, \beta) = \begin{cases} \mu + \frac{\sigma}{1-\alpha} F_\beta^{-1}\left(\frac{p}{2\alpha}\right) & , p \leq \alpha \\ \mu + \frac{\sigma}{\alpha} F_\beta^{-1}\left(\frac{1+p-2\alpha}{2(1-\alpha)}\right) & , p > \alpha \end{cases} \quad (12)$$

2.4 Empirical central normality test

Power transformations aim to transform features to a normal distribution. However, this may not always be successful or possible. Deviations from normality can be detected by normality tests, such as the Shapiro-Wilk test (Shapiro & Wilk, 1965). In practice, normality tests may be too stringent with large sample sizes, outliers, or both. Here we develop an empirical test for central normality.

Definition (Central portion of a sequence). Let $\mathbf{X} = \{x_1, x_2, \dots, x_n | x_i \in \mathbb{R}\}$ be a finite sequence of length $n > 0$, ordered so that $x_1 \leq x_2 \leq \dots \leq x_n$. Let $p_i = \frac{i-1/3}{n+1/3}$, with $i = 1, 2, \dots, n$ be the percentile value corresponding to each element in \mathbf{X} . For elements with tied values in \mathbf{X} , percentile values are replaced by the average in their group, i.e. if $x_j = x_{j+1} = \dots = x_{j+m}$, then $p'_j = p'_{j+1} = \dots = p'_{j+m} = 1/(m+1) \sum_j^{j+m} p_j$. Furthermore, let central portion $\kappa \in (0, 1)$.

Then the central portion of \mathbf{X} is $\mathbf{X}_c = \{x_i \in \mathbf{X} | \frac{1-\kappa}{2} \leq p_i \leq \frac{1+\kappa}{2}\}$.

Definition (Residual errors of the central portion of a sequence). *Let the residual error for each element of \mathbf{X} be $r_i = \left| \frac{x_i - \mu_M}{\sigma_M} - F_N^{-1}(p_i) \right|$, with μ_M and σ_M robust Huber M-estimates of location and scale of \mathbf{X} (Huber, 1981), and F_N^{-1} the quantile function of the normal distribution $\mathcal{N}(0, 1)$.*

Then, the set of residual errors of the central portion of \mathbf{X} (i.e. \mathbf{X}_c) is $\mathbf{R}_c = \{r_i \in \{r_1, r_2, \dots, r_n\} \mid \frac{1-\kappa}{2} \leq p_i \leq \frac{1+\kappa}{2}\}$.

Definition (Central normal distribution). *A central normal distribution is any distribution whose quantile function is defined by F_N^{-1} for $\frac{1-\kappa}{2} \leq p \leq \frac{1+\kappa}{2}$, with N any normal distribution.*

Corollary. *For $\kappa = 1.0$, the central normal distribution is a normal distribution.*

Corollary. *By the Glivenko-Cantelli theorem, if a sequence \mathbf{X} was sampled from a central normal distribution, then almost surely $\lim_{n \rightarrow \infty} \sum_{r_j \in \mathbf{R}_c} r_j = 0$,*

Definition (Central normality test). *The null-hypothesis H_0 is that the sequence \mathbf{X} was sampled from a population that is distributed according to a central normal distribution.*

The alternative hypothesis is that the sequence \mathbf{X} was sampled from a population that is not distributed according to a central normal distribution.

To test this hypothesis, a test statistic is computed and compared against a critical value.

Definition (Central normality test statistic). *Let m be the number of elements of \mathbf{R}_c .*

The test statistic is then $\tau_{n,\kappa} = \frac{1}{m} \sum_{r_j \in \mathbf{R}_c} r_j$.

The null-hypothesis should be rejected at significance level α if $\tau_{n,\kappa} \geq \tau_{\alpha,n,\kappa,\text{critical}}$. Critical test statistic values are determined in the [Simulation](#) section.

3 Simulation

We used simulated data to assess invariance to location and scale of the proposed power transformations, to develop the empirical central normality test, and to determine weighting for robust transformations. The λ parameter for conventional power transformations (Eqn. 1 and 2), as well as λ , x_0 and s parameters for location-and scale-invariant power transformations (Eqn. 3 and 4) were estimated using the BOBYQA algorithm for derivative-free bound constraint optimisation (Powell, 2009) through maximum likelihood estimation. The required algorithms were implemented in the `power.transform` R software package (Zwanenburg & Löck, 2025b) (version 1.0.2). Of note, the `power.transform` package shifts feature values into the positive domain if negative or zero values are present for Box-Cox power transformations.

3.1 Invariance to location and scale

To assess whether the proposed power transformations lead to values of λ that are invariant to location and scale of the distribution, we simulated three different sequences. We first randomly drew 10000 values from a normal distribution: $\mathbf{X}_{\text{normal}} = \{x_1, x_2, \dots, x_{10000}\} \sim \mathcal{N}(0, 1)$, or equivalently $\mathbf{X}_{\text{normal}} = \{x_1, x_2, \dots, x_{10000}\} \sim \mathcal{AGN}(0, 1/\sqrt{2}, 0.5, 2)$. The second distribution was a right-skewed generalised normal

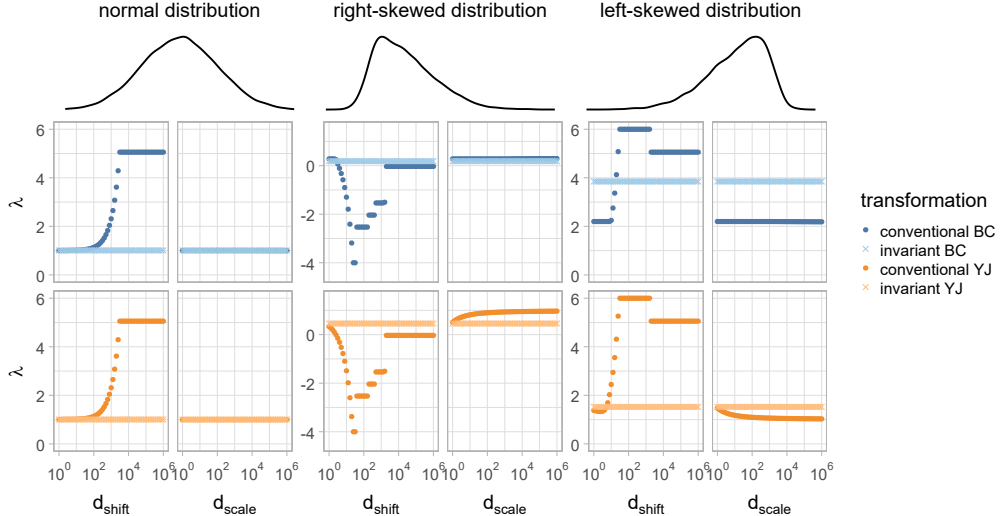


Fig. 3 Invariant power transformation produces transformation parameters that are invariant to location and scale. Samples were drawn from normal, right-skewed and left-skewed distributions, respectively, which then underwent a shift d_{shift} or multiplication by d_{scale} . Estimates of the transformation parameter λ for the conventional power transformations show strong dependency on the overall location and scale of the distribution, whereas estimates obtained for the location- and scale-invariant power transformations are constant.

distribution $\mathbf{X}_{\text{right}} = \{x_1, x_2, \dots, x_{10000}\} \sim \mathcal{AGN}(0, 1/\sqrt{2}, 0.2, 2)$. The third distribution was a left-skewed generalised normal distribution $\mathbf{X}_{\text{left}} = \{x_1, x_2, \dots, x_{10000}\} \sim \mathcal{AGN}(0, 1/\sqrt{2}, 0.8, 2)$. We then computed transformation parameter λ using the original definitions (Eqn. 1 and 2) and the location- and scale-invariant definitions (Eqn. 3 and 4) for each distribution. To assess location invariance, a positive value d_{shift} was added to each distribution with $d_{\text{shift}} \in [1, 10^6]$. Similarly, to assess scale invariance, each distribution was multiplied by a positive value d_{scale} , where $d_{\text{scale}} \in [1, 10^6]$.

The result is shown in Figure 3. For each distribution, transformation parameter λ varied with d_{shift} and d_{scale} when estimated for conventional transformations. In contrast, estimation of λ for invariant power transformations was invariant to both d_{shift} and d_{scale} .

3.2 Empirical central normality test

The critical test statistic for the empirical central normality test depends on the significance level α , sequence length n and central portion κ . Critical test statistic values were set through simulation, as described below.

For each number of samples $n \in \{\lfloor 10^\nu \rfloor | \nu \in \{0.7500, 0.8125, \dots, 4.0000\}\}$ we randomly sampled $m_d = 30000$ ordered sequences \mathbf{X} from $\mathcal{N}(0, 1)$. For each sequence we then computed τ_κ for $\kappa \in \{0.50, 0.60, 0.70, 0.80, 0.90, 0.95, 1.00\}$.

Figure 4 shows the critical test statistic $\tau_{\alpha, n, \kappa}$ as a function of n for different values of κ and α . For larger central portion κ , critical test statistic values increase. Similarly, critical test statistic values increase for lower significance levels.

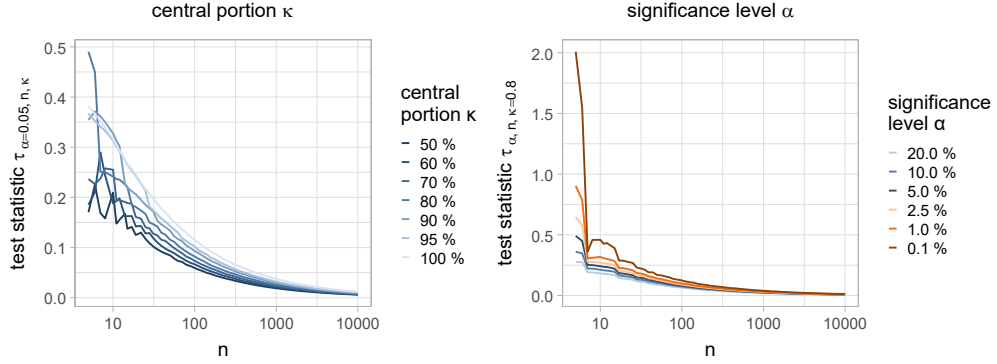


Fig. 4 Critical test statistic $\tau_{\alpha=0.05,n,\kappa}$ of the empirical central normality test as function of n for several values of central portion κ (left) and several values of significance level α (right).

To assess type I error rates for the empirical central normality test and compare these to the Shapiro-Wilk test for normality, we randomly drew another 10000 sequences from a central normal distribution for each $n \in \{\lfloor 10^\nu \rfloor | \nu \in \{0.7500, 0.8125, \dots, 3.0000\}\}$.

Each sequence was created as follows: first n values are sampled from $\mathcal{N}(0, 1)$. Then, the elements outside the central portion of the sequence (i.e. $\mathbf{X} \setminus \mathbf{X}_c$) are replaced. Elements with $p_i < \frac{1-\kappa}{2}$ are replaced with values sampled from $\mathcal{U}(-10, \min(\mathbf{X}_c))$, and elements with $p_i > \frac{1+\kappa}{2}$ are replaced with values sampled from $\mathcal{U}(\max(\mathbf{X}_c), 10)$.

For each sequence, the p-value for the respective test was used to reject the null hypothesis that sequences were derived from a population with a (central) normal distribution. The null hypothesis was rejected if $p \leq 0.05$. The type I error rate was determined by computing the fraction of sequences rejected this way. Figure 5 shows that when the central portion κ of the central normal distribution is equal or greater than the κ parameter for the empirical central normality test, the tests are accurate. If κ of the empirical central normality test exceeds that the central portion κ for the underlying distribution, tests are conservative. The Shapiro-Wilk test behaves similar to the empirical central normality test with $\kappa = 1.0$, which is expected. For $n < 10$, the empirical central normality test can be optimistic.

In Figure 6 we apply the empirical central normality test (with $\kappa = 0.80$) to assess central normality of features that are composed of a mixture of samples drawn from two normal distributions ($n = 100$ each). With increased separation of the underlying normal distributions, the test's p-value decreases, as expected.

We use $\kappa = 0.80$ for the empirical central normality tests in the remainder of the manuscript, unless noted otherwise. Critical statistic values of the empirical central normality test for $\kappa = 0.80$ are shown in Table C1.

3.3 Robust transformations

Outliers may be present in data and affect estimation of transformation parameters. The log-likelihood function can be weighted to assign less weight to outlier instances, see equations 7 and 8. We propose three weighting functions: step, triangle and tapered cosine, that have one, two and two parameters, respectively. Each weighting function

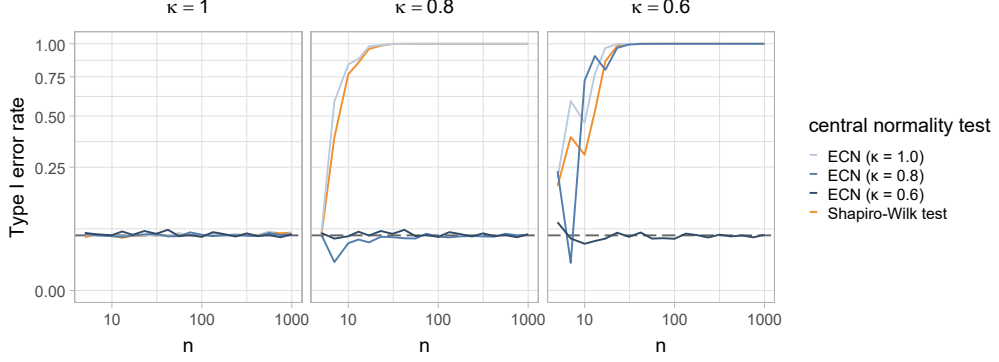


Fig. 5 Observed type I error rates for central normality tests in the presence of data sampled from central normal distributions with $\kappa \in \{0.6, 0.8, 1.0\}$. Three empirical central normality (ECN) tests were performed, parameterised with same value for the central portion κ . Additionally, the Shapiro-Wilk test was assessed. The dashed line indicates the expected type I error rate for rejecting the null hypothesis at significance level $\alpha = 0.05$. ECN: empirical central normality

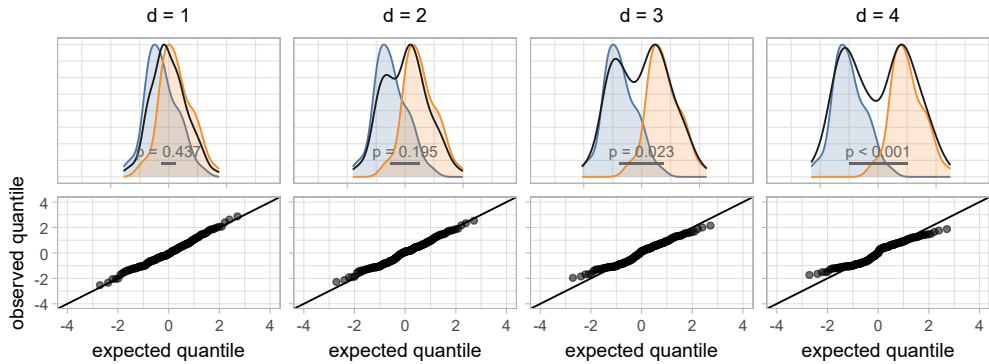


Fig. 6 Bi-modal distributions and empirical central normality test results. The feature (black) is a mixture of two identical sample sets (blue and orange, $n = 100$) drawn from normal distributions that are offset by a distance d . The empirical central normality test ($\kappa = 0.80$) is used to test the hypothesis that the mixture is sampled from a central normal distribution. As may be observed, with increasing offset d the test's p-value decreases. Quantile-quantile plots are drawn below each distribution.

then uses one of the following inputs: probabilities of the empirical distribution of the original feature, the z-score of the transformed feature values, or the residual error between the z-score of the transformed feature values and their expected z-score based on the normal distribution.

To determine the weighting function parameters for each of the nine combinations, $m_d = 500$ sequences \mathbf{X}_i ($i \in \{1, 2, \dots, m_d\}$) were randomly drawn from randomly parametrised asymmetric generalised normal distributions. Each distribution was parametrised with a random skewness parameter $\alpha \sim U(0.01, 0.99)$ and shape parameter $\beta \sim U(1.00, 5.00)$. Location and scale parameters were set as $\mu = 0$ and $\sigma = 1$, respectively. To form each sequence \mathbf{X}_i , $n = \lceil 10^\gamma \rceil$ instances were then randomly drawn, with $\gamma \sim U(\log_{10} 50, 3)$, resulting in a set of sequences with between 50 and 1000 elements each. Outlier values were then drawn to randomly replace 10

Table 1 Optimal weighting parameters and corresponding loss for location- and scale-invariant Box-Cox power transformations. p^* indicates use of the empirical distribution of feature values, z the z-score of the transformed feature values, and r the residual error between the z-score of transformed feature values and the expected z-score according to the normal distribution. The *initial* column shows the starting parameter value for the optimisation process, with the corresponding boundary values in the *limits* column. The *optimal* column shows the optimal parameter values. The *loss* column shows the composite loss achieved by each method under optimised parameters. This loss is based on residual errors of transformed features and deviations in λ parameters found compared to the λ parameters found prior to inserting outliers. The loss metric can be compared between different weighting methods.

method	δ_1		δ_2		loss	
	initial	limits	optimal	initial	limits	
non-robust	—	—	—	—	—	49.6
p^* (step)	0.80	(0, 1]	0.80	—	—	38.5
p^* (triangle)	0.80	(0, 1]	0.01	1.00	(0, 1]	0.86
p^* (tapered cosine)	0.80	(0, 1]	0.00	1.00	(0, 1]	0.90
z (step)	1.28	(0, 10]	2.39	—	—	52.2
z (triangle)	1.28	(0, 10]	2.39	2.40	(0, 10]	4.92
z (tapered cosine)	1.28	(0, 10]	1.07	3.63	(0, 10]	3.43
r (step)	0.50	(0, 10]	0.83	—	—	53.1
r (triangle)	0.50	(0, 10]	0.80	0.81	(0, 10]	0.84
r (tapered cosine)	0.50	(0, 10]	0.76	0.77	(0, 10]	0.76
						53.2

percent of the elements of \mathbf{X}_i . These values were set according to Tukey (1977), as follows. Let $x^* \sim U(-2, 2)$. Then the corresponding outlier value was:

$$x_{out} = \begin{cases} Q_1 - (1.5 - x^*) \text{IQR} & \text{if } x^* < 0 \\ Q_3 + (1.5 + x^*) \text{IQR} & \text{if } x^* \geq 0 \end{cases} \quad (13)$$

Here, Q_1 , Q_3 and IQR are the first quartile, third quartile and interquartile range of \mathbf{X}_i , respectively.

To find the optimal values for the weighting function parameters δ_1 and δ_2 (if applicable), we minimised a composite loss $L = \sum_{i=1}^{m_d} L_{cn,i} + 0.1 \sum_{i=1}^{m_d} L_{\lambda,i}$. The composite loss consisted of two components: a loss term $L_{cn,i} = \tau_{n_i, \kappa=0.80, i}$, i.e. the mean of residual errors of the central 80% of elements of each sequence \mathbf{X}_i , which aimed at optimising central normality; and a loss term $L_{\lambda,i} = \max(0.0, |\lambda_{0,i} - \lambda_i| - \xi)$, with $\lambda_{0,i}$ and λ_i transformation parameters found for sequence \mathbf{X}_i prior to and after adding outliers, respectively, and tolerance parameter $\xi = 0.5$ for Box-Cox and $\xi = 0.3$ for Yeo-Johnson power transformations. This second term aimed to prevent solutions that provide small improvements in central normality at the cost of a poor fit of the tails of sequences.

Minimisation was conducted using the BOBYQA algorithm for derivative-free bound constraint optimisation (Powell, 2009). The resulting weighting function parameters for weighted MLE are shown in Tables 1 and 2 for robust location- and scale-invariant Box-Cox and Yeo-Johnson transformations, respectively.

Table 2 Optimal weighting parameters and corresponding loss for location- and scale-invariant Yeo-Johnson power transformations. p^* indicates use of the empirical distribution of feature values, z the z-score of the transformed feature values, and r the residual error between the z-score of transformed feature values and the expected z-score according to the normal distribution. The *initial* column shows the starting parameter value for the optimisation process, with the corresponding boundary values in the *limits* column. The *loss* column shows the composite loss achieved by each method under optimised parameters. This loss is based on residual errors of transformed features and deviations in λ parameters found compared to the λ parameters found prior to inserting outliers. The loss metric can be compared between different weighting methods.

method	δ_1		δ_2		loss	
	initial	limits	optimal	initial	limits	
non-robust	—	—	—	—	—	42.1
p^* (step)	0.80	(0, 1]	0.78	—	—	35.1
p^* (triangle)	0.80	(0, 1]	0.20	0.95	(0, 1]	1.00
p^* (tapered cosine)	0.80	(0, 1]	0.54	0.95	(0, 1]	1.00
z (step)	1.28	(0, 10]	2.32	—	—	43.0
z (triangle)	1.28	(0, 10]	1.28	1.96	(0, 10]	3.43
z (tapered cosine)	1.28	(0, 10]	0.41	1.96	(0, 10]	3.75
r (step)	0.50	(0, 10]	0.92	—	—	65.4
r (triangle)	0.50	(0, 10]	0.87	1.00	(0, 10]	0.87
r (tapered cosine)	0.50	(0, 10]	1.06	1.00	(0, 10]	1.07
						67.1

3.4 Assessing transformations using simulated data

Three datasets with 100000 sequences each were created to assess transformation to normality. For each sequence \mathbf{X}_i , $n = \lceil 10^\gamma \rceil$ elements were randomly drawn, with $\gamma \sim U(1, 4)$, resulting in sequences with between 10 and 10000 elements.

- A *clean* dataset with each sequence drawn from $\mathcal{N}(0, 1)$ and transformed using an inverse power transformation with randomly drawn transformation parameter $\lambda \sim U(0.00, 2.00)$. $(\phi_{BC}^\lambda)^{-1}$ and $(\phi_{YJ}^\lambda)^{-1}$ were used as inverse transformations for assessing Box-Cox and Yeo-Johnson transformations, respectively. Prior to inverse transformation, sequences for Box-Cox transformations were shifted into the positive domain, with minimum value 1.
- A *dirty* dataset with each sequence drawn from $\mathcal{AGN}(\mu = 0, \sigma = 1/\sqrt{2}, \alpha, \beta)$, with randomly drawn skewness parameter $\alpha \sim U(0.01, 0.99)$ and shape parameter $\beta \sim U(1.00, 5.00)$.
- A *shifted* dataset with each sequence drawn from $\mathcal{AGN}(\mu = 100, \sigma = 10^{-3} \cdot 1/\sqrt{2}, \alpha, \beta)$, with randomly drawn skewness parameter $\alpha \sim U(0.01, 0.99)$ and shape parameter $\beta \sim U(1.00, 5.00)$.

A dataset with outliers was created for each of the above datasets by replacing 10 percent of elements in each sequence, as described earlier.

In addition to no power transformation and location- and scale-invariant power transformations, conventional and Raymaekers and Rousseeuw's robust adaptation (Raymaekers & Rousseeuw, 2024) were assessed. For the latter two methods, normalisation before standardisation using was additionally assessed using the following two methods:

Table 3 Comparison of average rank between Yeo-Johnson transformation methods based on either residual error (without outliers) or residual error of the central portion (with outliers; $\kappa = 0.80$) over 3 datasets with 100000 sequences each. The clean dataset consists of sequences derived through inverse Yeo-Johnson transformation of data sampled from a standard normal distribution. The dirty dataset contains sequences sampled from asymmetric generalised normal distributions, centred at 0. The shifted dataset also contains sequences sampled from asymmetric generalised normal distributions, but centred at 100, and scaled by 0.001. Several transformation methods include normalisation before transformation, indicated by z-score normalisation (norm.) or robust scaling. A rank of 1 is the best and a rank of 9 the worst. For each dataset, the best ranking transformation is marked in bold.

transformation	dataset: outliers:	clean		dirty		shifted	
		no	yes	no	yes	no	yes
none		8.52	7.62	7.35	6.17	7.46	6.62
conventional		3.82	5.78	3.86	7.08	6.51	5.95
conventional (z-score norm.)		4.70	5.75	6.44	5.07	5.48	4.93
conventional (robust scaling)		3.83	6.61	5.36	5.72	4.41	5.59
Raymaekers-Rousseeuw		4.64	3.22	4.01	4.11	6.28	5.67
Raymaekers-Rousseeuw (z-score norm.)		5.24	2.66	6.25	3.62	5.29	3.50
Raymaekers-Rousseeuw (robust scaling)		4.70	2.99	5.22	3.69	4.27	3.57
invariant		3.11	6.74	3.24	6.13	2.63	6.03
robust invariant		6.44	3.64	3.27	3.40	2.65	3.14

1. z-standardisation: $x'_i = (x_i - \mu) / \sigma$, with μ and σ the mean and standard deviation of sequence \mathbf{X} .
2. robust scaling: $x'_i = (x_i - \text{median}(\mathbf{X})) / Q_n(\mathbf{X})$, with Q_n representing the robust Q_n scale estimator of \mathbf{X} (Croux & Rousseeuw, 1992; Rousseeuw & Croux, 1993).

This results in nine types of power transformation. Transformation parameters were optimised for each sequence. Subsequently the sum of residual errors and sum of residual errors of the central portion ($\kappa = 0.80$) were computed for each sequence after transformation. Then, each method was ranked according to the sum of residual errors (data without outliers) or the sum of residual errors of the central portion (data with outliers). The average rank of each transformation method was computed over all 100000 sequences in each dataset. Average ranks for Yeo-Johnson transformations are shown in Table 3. Location and shift-invariant Yeo-Johnson transformation ranked best for all datasets without outliers. The robust variant ranked best in dirty and shifted datasets with outliers, but not in the clean dataset. Results for Box-Cox transformations are shown in Table D2.

4 Experimental Results

4.1 Invariance

Location- and scale-invariant power transformations are intended to yield improved transformations to normality in the presence of large shifts in location, distributions that due to location and scale are not centered near zero, or both. Earlier, we assessed these transformations using simulated data. In the following, they are evaluated using examples from real datasets. We focus on the Yeo-Johnson transformation because of

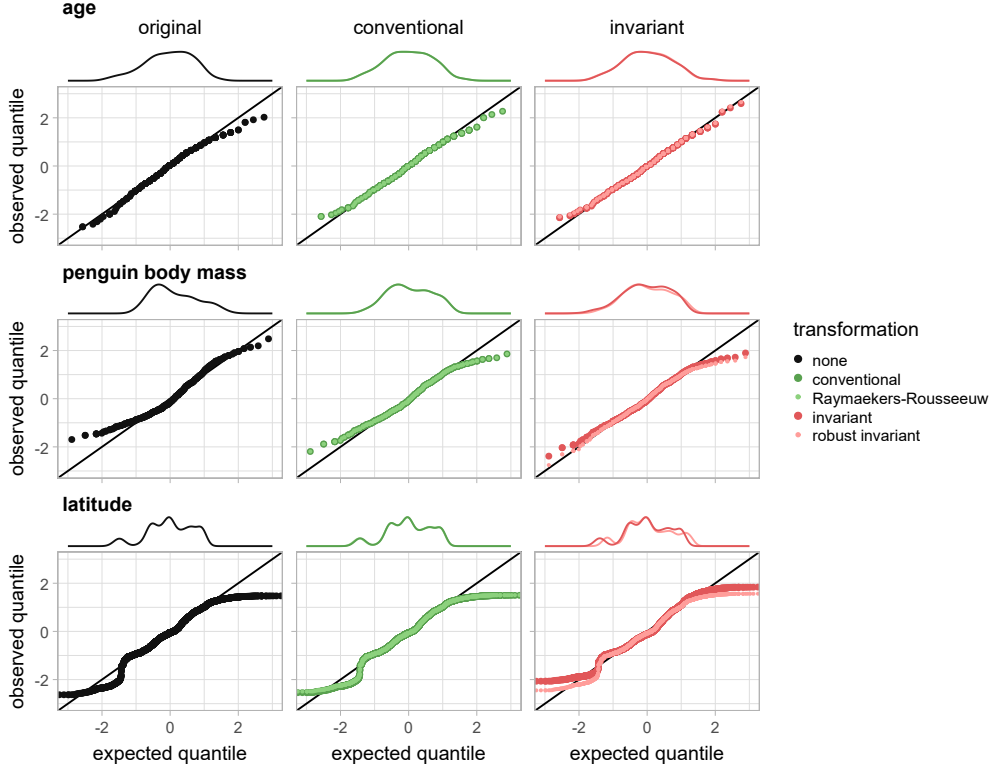


Fig. 7 Quantile-quantile plots for several datasets: age of patients with lung cancer (top row); penguin body mass (middle row); and latitude coordinates of houses sold in Ames, Iowa (bottom row). Multiple quantile-quantile plots are shown: for the original feature (left column); the feature transformed using the conventional Yeo-Johnson transformation and Raymaekers and Rousseeuw’s robust adaptation (middle column); and the feature transformed using the non-robust and robust location- and scale-invariant Yeo-Johnson transformations (right column).

its ability to handle features with negative values. Results for Box-Cox transformations are shown in [Appendix D](#).

4.1.1 Age of patients with lung cancer

A common feature in health-related datasets is age. Here we use data on 228 patients with lung cancer that was collected and published by Loprinzi et al. ([Loprinzi et al., 1994](#)). The age in the cohort was 62.4 ± 9.1 (mean \pm standard deviation) years. Applying conventional and invariant Yeo-Johnson transformations to patient age yielded the following results, see Figure 7: no transformation ($\sum r_i = 16.5$, $p = 0.54$); conventional transformation ($\lambda = 2.0$, $\sum r_i = 11.5$, $\mu_{YJ} = 1.8 \cdot 10^3$, $\sigma_{YJ} = 0.5 \cdot 10^3$, $p = 0.92$); Raymaekers and Rousseeuw’s robust adaptation ($\lambda = 2.0$, $\sum r_i = 11.5$, $\mu_{YJ} = 1.8 \cdot 10^3$, $\sigma_{YJ} = 0.5 \cdot 10^3$, $p = 0.92$); location- and scale-invariant transformation ($\lambda = 1.3$, $\sum r_i = 8.8$, $\mu_{YJ} = -1.2$, $\sigma_{YJ} = 1.1$, $p = 0.95$); and robust location- and scale-invariant transformation ($\lambda = 1.3$, $\sum r_i = 9.3$, $\mu_{YJ} = -1.0$, $\sigma_{YJ} = 1.1$, $p = 0.87$).

Location- and scale-invariant transformation led to a lower overall residual error, indicating a better transformation to normality. Conventional transformations inflated the mean μ_{YJ} and standard deviation σ_{YJ} of the age feature after transformation. The empirical central normality test did not detect any statistically significant deviations from central normality for any transformation (all $p \geq 0.87$).

4.1.2 Penguin body mass

Gorman, Williams and Fraser recorded body mass (in grams) of 342 penguins of three different species ([Gorman, Williams, & Fraser, 2014](#)). The body mass was $(4.2 \pm 0.8) \cdot 10^3$ (mean \pm standard deviation) grams, and not centrally normal ($p < 0.001$). Applying conventional and invariant Yeo-Johnson transformations to body mass yielded the following results, see Figure 7: no transformation (residual sum $\sum r_i = 48.0$, $p < 0.001$); conventional transformation ($\lambda = -0.5$, $\sum r_i = 32.2$, $\mu_{YJ} = 2.1$, $\sigma_{YJ} = 4 \cdot 10^{-3}$, $p = 0.03$); Raymaekers and Rousseeuw's robust adaptation ($\lambda = -0.5$, $\sum r_i = 32.2$, $\mu_{YJ} = 2.1$, $\sigma_{YJ} = 4 \cdot 10^{-3}$, $p = 0.03$); location- and scale-invariant transformation ($\lambda = 0.5$, $\sum r_i = 26.8$, $\mu_{YJ} = 0.9$, $\sigma_{YJ} = 0.9$, $p = 0.12$); and robust location- and scale-invariant transformation ($\lambda = 0.3$, $\sum r_i = 22.0$, $\mu_{YJ} = 0.7$, $\sigma_{YJ} = 0.9$, $p = 0.48$).

Location- and scale-invariant transformation yielded lower overall residual errors, indicating a better transformation to central normality, which is reflected by the empirical central normality test results. Conventional transformations led to low standard deviation σ_{YJ} of the body mass feature after transformation, and the null hypothesis of the empirical central normality test was rejected (at significance level $\alpha = 0.05$) in both cases.

4.1.3 Latitude in the Ames housing dataset

Geospatial datasets usually contain coordinates. The Ames housing dataset contains data on 2930 properties that were sold between 2006 and 2010 ([De Cock, 2011](#)), including their geospatial coordinates. The latitude was 42.03 ± 0.02 (mean \pm standard deviation). Applying conventional and invariant Yeo-Johnson transformations to latitude yielded the following results, see Figure 7: no transformation (residual sum $\sum r_i = 328$, $p < 0.001$); conventional transformation ($\lambda = 62.1$, $\sum r_i = 319$, $\mu_{YJ} = 4.8 \cdot 10^{99}$, $\sigma_{YJ} = 0.1 \cdot 10^{99}$, $p < 0.001$); Raymaekers and Rousseeuw's robust adaptation ($\lambda = 95.4$, $\sum r_i = 315$, $\mu_{YJ} = 6.4 \cdot 10^{153}$, $\sigma_{YJ} = 0.3 \cdot 10^{153}$, $p < 0.001$); location- and scale-invariant transformation ($\lambda = 1.5$, $\sum r_i = 326$, $\mu_{YJ} = -1.2$, $\sigma_{YJ} = 0.8$, $p < 0.001$); and robust location- and scale-invariant transformation ($\lambda = 1.1$, $\sum r_i = 308$, $\mu_{YJ} = -1.3$, $\sigma_{YJ} = 1.2$, $p < 0.001$).

Every transformation reduced the residual sum compared to the original data. None of the transformations yielded a centrally normal distribution. Conventional transformations had high values for the λ parameter, which could lead to numerical issues.

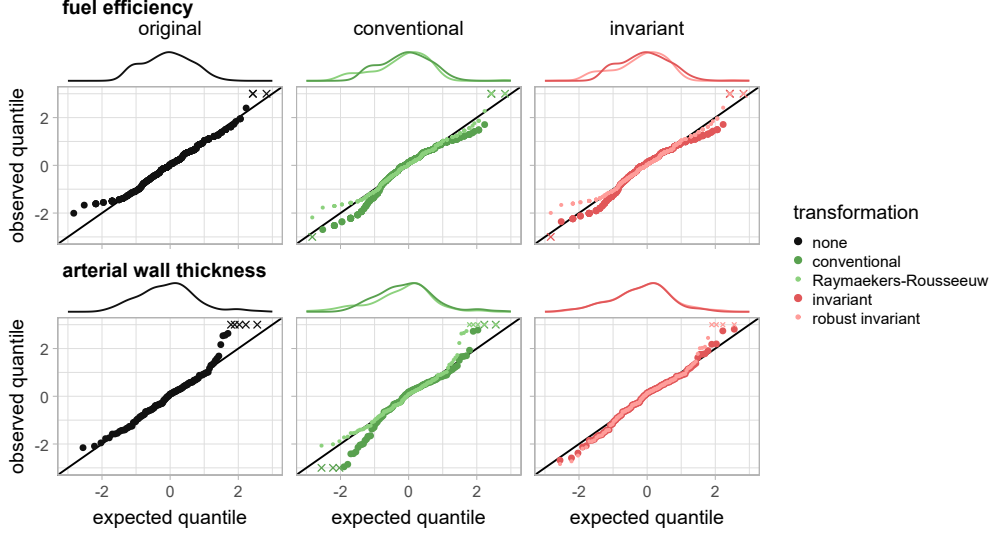


Fig. 8 Quantile-quantile plots for two datasets with outliers: vehicle fuel consumption (top row), where outliers are related to highly fuel-efficient vehicles; and maximum arterial wall thickness in patients with ischemic stroke (bottom row). Multiple quantile-quantile plots are shown: for the original feature (left column); the feature transformed using the conventional Yeo-Johnson transformation and Raymaekers and Rousseeuw’s robust adaptation (middle column); and the feature transformed using the non-robust and robust location- and scale invariant Yeo-Johnson transformations (right column). Samples with observed quantiles below -3.0 or above 3.0 are indicated by crosses.

4.2 Robustness against outliers

We previously simulated data to assess invariant power transformations and their robustness against outliers. Here, we assess invariant power transformations in real data with outliers.

4.2.1 Fuel efficiency in the Top Gear dataset

The Top Gear dataset contains data on 297 vehicles that appeared on the BBC television show *Top Gear* (Alfons, 2021). Within this dataset, the fuel consumption feature contains outliers due to highly fuel-efficient vehicles. Applying conventional and invariant Yeo-Johnson transformations to the fuel consumption feature yielded the following results, see Figure 8: no transformation (residual sum $\sum r_i = 54$, $p = 0.55$); conventional transformation ($\lambda = -0.1$, $\sum r_i = 55$, $\mu_{YJ} = 3.0$, $\sigma_{YJ} = 0.3$, $p < 0.001$); Raymaekers and Rousseeuw’s robust adaptation ($\lambda = 0.8$, $\sum r_i = 48$, $\mu_{YJ} = 29$, $\sigma_{YJ} = 15$, $p = 0.21$); location- and scale-invariant transformation ($\lambda = -1.3$, $\sum r_i = 44$, $\mu_{YJ} = 0.5$, $\sigma_{YJ} = 0.1$, $p < 0.001$); and robust location- and scale-invariant transformation ($\lambda = 1.0$, $\sum r_i = 56$, $\mu_{YJ} = 1.7$, $\sigma_{YJ} = 1.0$, $p = 0.59$).

Outliers caused non-robust transformations to fail the empirical central normality test for transforming the feature to a centrally normal distribution.

4.2.2 Maximum arterial wall thickness in an ischemic stroke dataset

The ischemic stroke dataset contains historic data from 126 patients with risk at ischemic stroke ([Kuhn & Johnson, 2019](#)). These patients underwent Computed Tomography Angiography to characterize the carotid artery blockages. Angiography imaging was then assessed, and various characteristics related to the blood vessels and the disease are measured. The maximum arterial wall thickness feature contains several instances with outlier values. Applying conventional and invariant Yeo-Johnson transformations to this feature yielded the following results, see Figure 8: no transformation (residual sum $\sum r_i = 110$, $p = 0.73$); conventional transformation ($\lambda = -0.7$, $\sum r_i = 30$, $\mu_{YJ} = 1.0$, $\sigma_{YJ} = 0.1$, $p < 0.001$); Raymaekers and Rousseeuw's robust adaptation ($\lambda = 1.1$, $\sum r_i = 136$, $\mu_{YJ} = 7.2$, $\sigma_{YJ} = 14.3$, $p = 0.80$); location-and scale-invariant transformation ($\lambda = 0.2$, $\sum r_i = 12$, $\mu_{YJ} = -11.8$, $\sigma_{YJ} = 6.9$, $p = 0.07$); and robust location- and scale-invariant transformation ($\lambda = -0.3$, $\sum r_i = 30$, $\mu_{YJ} = 0.8$, $\sigma_{YJ} = 0.2$, $p = 0.09$).

For conventional non-robust transformation the null hypothesis was rejected (at $\alpha = 0.05$), indicating that they failed to produce a transformed feature that followed a central normal distribution.

4.3 Integration into end-to-end machine learning

We used 231 datasets containing at least one numeric feature from the Penn Machine Learning Benchmarks collection ([Romano et al., 2022](#)). In this collection, 114 datasets correspond to regression tasks and 117 datasets to classification tasks. Using the familiar auto-machine learning library ([Zwanenburg & Löck, 2025a](#)) (version 1.5.0), each dataset was used to train a model for each of 32 process configurations. Each process configuration specifies the learner (generalised linear model, L1-regularised linear models (Lasso), gradient boosted linear model, or random forest), transformation method (none, conventional Yeo-Johnson, robust invariant Yeo-Johnson, robust invariant Yeo-Johnson with empirical central normality test (rejecting transformations with $p \leq 0.01$), and normalisation method (none, z -standardisation), yielding 32 distinct configurations. Before each experiment, each dataset was randomly split into a training (70%) and holdout test (30%) set five times. Thus, a total of 36960 models were created. Each model was then evaluated using the holdout test set using one of two metrics, i.e. the root relative squared error (RRSE) for regression tasks and the area under the receiver operating characteristic curve (AUC) for classification tasks.

For the purpose of assessing the effect of the difficulty of the task, we computed the median performance score over all models for each dataset and assigned one the following categories:

- very easy: $AUC \geq 0.90$ or $RRSE \leq 0.10$ (57 datasets)
- easy: $0.90 > AUC \geq 0.80$ or $0.30 \geq RRSE > 0.10$ (40 datasets)
- intermediate: $0.80 > AUC \geq 0.70$ or $0.60 \geq RRSE > 0.30$ (52 datasets)
- difficult: $0.70 > AUC \geq 0.60$ or $0.80 \geq RRSE > 0.60$ (33 datasets)
- very difficult: $0.60 > AUC \geq 0.50$ or $1.00 \geq RRSE > 0.80$ (48 datasets)
- unsolvable: $AUC < 0.50$ or $RRSE > 1.00$ (1 dataset)

To remove the effect of the dataset, and allow for comparing metrics, we ranked all performance scores for each dataset so that a higher rank corresponds to better performance. Experiments yielding the same score received the same, average, rank. Subsequently ranks were normalised to the $[0.0, 1.0]$ range.

Significant differences exist between process configurations (Friedman test: $p < 10^{-8}$).

Considering single process parameters, the choice of learner (Friedman test: $p < 10^{-8}$), normalisation method (Wilcoxon signed rank test: $p = 4 \cdot 10^{-8}$), and transformation method (Friedman test: $p = 0.007$), all had a significant impact (at $p = 0.05$).

To estimate the marginal effects of process parameters, including transformation method, we first fit a regression random forest (ranger package ([Wright & Ziegler, 2017](#)) version 0.16.0): 2000 trees, node size 2, other hyperparameters default) with process parameters and task difficulty as predictors and normalised rank as response variable. The estimated marginal effects are shown in Figure 9. On the scale of normalised ranks ($[0.0, 1.0]$), only the random forest performed better than the average of all learners (rank difference 0.173). The marginal improvement in performance from z-standardisation was 0.011. Transformation methods had the following marginal effects: -0.001 for using conventional Yeo-Johnson transformation instead of no transformation; -0.012 for using robust invariant Yeo-Johnson transformation instead of no transformation; -0.012 for using robust invariant Yeo-Johnson transformation with empirical central normality test instead of no transformation; -0.012 for using robust invariant Yeo-Johnson transformation instead of conventional Yeo-Johnson transformation; and -0.012 for using robust invariant Yeo-Johnson transformation with empirical central normality test instead of conventional Yeo-Johnson transformation.

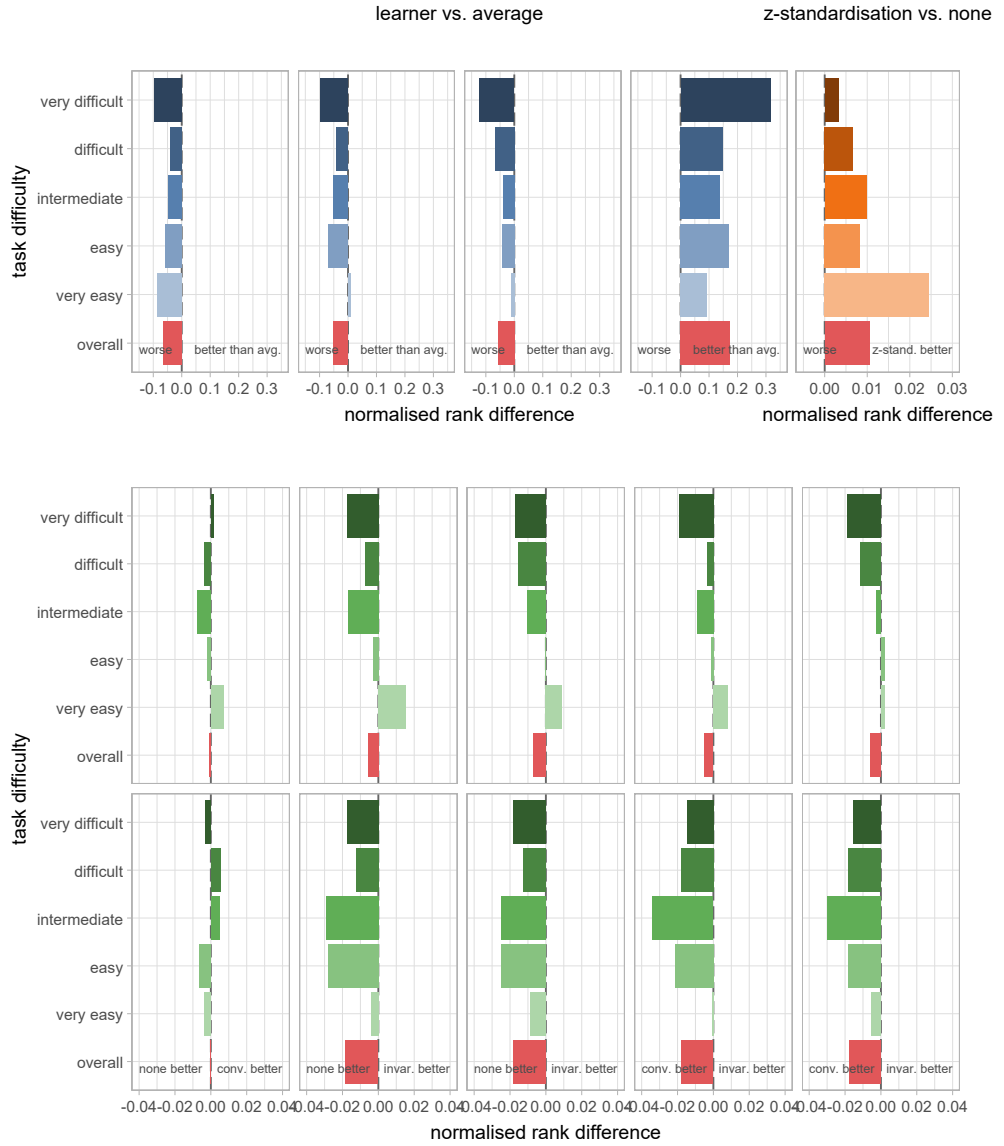


Fig. 9 Estimated marginal effect of learners, normalisation and transformation methods on ranked model performance scores in 36960 machine learning experiments on 231 datasets. The four top-left panels shows the marginal effect of learners vs. the average, i.e. generalised linear models (GLM), L1-regularised LM (Lasso), gradient-boosted LM and random forest. Random forests outperform the average. The top-right panel shows the marginal effect of feature normalisation methods, i.e. no normalisation and z-standardisation. z-standardisation is generally beneficial, but the estimated effect is marginal. The bottom panel shows the marginal effects of different transformation methods, split by normalisation method. The estimated effects are similar in size to the effect of normalisation and marginal. Note that the ranges of the x-axes of the three main panels differ. ECNT: empirical central normality test.

5 Discussion

In their work on power transformation, Box and Cox already mention transformation with a shift parameter, but preferred the version in Eq. 1 for the theoretical analysis in their paper ([Box & Cox, 1964](#)), which subsequently became the convention. Yeo and Johnson’s power transformation lacks a shift parameter altogether ([Yeo & Johnson, 2000](#)). We showed that these power transformations are sensitive to location and scale of data distributions. To mitigate this issue, we defined location- and scale-invariant variants of the Box-Cox and Yeo-Johnson transformations. We furthermore assessed methods for making these transformations robust to outliers, and devised an empirical test for central normality.

Robust location- and scale-invariant transformations are a suitable replacement for their conventional counterparts. They demonstrated robustness against outliers and prevent inaccurate transformations and potential numerical issues due to location and scale of the distribution of a feature. This is particularly relevant for automated data processing, where such issues may go unnoticed.

In simulation, robust location- and scale-invariant transformations ranked best in datasets with outliers, and ranked highly in datasets without outliers, except for features without outliers that were directly sampled from strictly normal distributions. In real-world examples, robust location-and scale-invariant transformations achieved central normality when the non-robust variant could not.

However, in a machine learning experiment of 231 real-world datasets that contained at least one numeric feature, we did not find a meaningful benefit – nor detriment – to model performance for location- and scale-invariant power transformations. One reason may be that numeric features with large location shifts ($|\mu| > 1000.0$) were uncommon. Of the 4886 numeric features in the 231 datasets, 266 (5%) features in 34 datasets had large location shifts, of which 200 appeared in just 2 datasets. For the latter two datasets, the transformation method did not show significant difference between groups (Friedman test; $p > 0.05$).

Location- and scale-invariant transformations are realised by simultaneously optimising three parameters, i.e. transformation parameter λ , shift parameter x_0 and scale parameter s . We derived the log-likelihood function to facilitate optimisation using MLE. Alternatively, standardisation of a numeric feature (e.g., through subtracting its median value and division by its interquartile range) prior to conventional power transformations can achieve a similar effect in reducing sensitivity to the feature’s location and scale. While this alternative helps prevent these issues – provided that standardisation does not lead to negative values for Box-Cox transformations – location- and scale-invariant transformations are able to achieve better transformations to normality, as demonstrated by lower residual errors in simulation experiments.

We assessed several weighting methods to achieve robust power transformations. Robust power transformations should satisfy two conflicting aims: they should minimise residual errors after transformation to central normality, and minimise the overall effect of outliers on estimation of transformation parameter λ . These aims are reflected in the composite loss used to optimise weighting parameters. For Yeo-Johnson transformation, empirical probabilities with tapered cosine weighting resulted in the lowest loss. The optimal parameters led to weights that gradually decline towards the

tails of empirical probabilities, i.e. elements with low and high values receive less or no weight. Similarly, for Box-Cox transformation, empirical probabilities with step weighting resulted in the lowest loss. In this case the central 80% of the elements are used, and the remaining 10% in each tail are ignored. Methods that relied on the z-score of the transformed feature or the residual error yielded worse loss than the non-robust method or those based on empirical probabilities. Underperformance of these weighting methods could be explained by their reliance on transformed feature values for setting weights. Consequently, their weights change at each iteration in the MLE optimisation process. This increases local variance in the log-likelihood function and creates local optima that the optimiser may not handle well. Methods that relied on the empirical probability did not suffer from this issue, as weights remained fixed during MLE.

We introduced an empirical test for central normality to assess whether sequences deviate from normality in a way that might require closer inspection prior to further processing. The empirical central normality test differs from other tests for normality, such as the Shapiro-Wilk test (Shapiro & Wilk, 1965), as it assesses normality of the central portion of a feature, instead of the entire feature. Compared to the Shapiro-Wilk test, the empirical central normality test remains consistent when a feature was not sampled from a normal distribution, such as a central normal distribution with $\kappa < 1.0$. This enables assessing reasonable normality of (transformed) features in the presence of outliers.

This work has the following limitation: We observed several numerical stability issues for optimisation criteria other than MLE (Appendix B). These appear in regions where transformation parameters would lead to very large or small numbers when using conventional power transformations. For MLE stability issues were not observed.

6 Conclusion

Compared to their conventional versions, robust location- and scale-invariant Box-Cox and Yeo-Johnson transformations reduce sensitivity to outliers and the location and scale of features. An empirical central normality test can assess the quality of transformation of features to normal distributions. The combination of both facilitate the use of power transformations in automated data analysis workflows.

Declarations

- Funding: No funding was received for conducting this study.
- Competing interests: The authors have no relevant financial or non-financial interests to disclose.
- Ethics approval and consent to participate: Not applicable
- Consent for publication: Not applicable
- Data availability: Data and results for the machine learning experiment are available from Zenodo (<https://doi.org/10.5281/zenodo.14986689>). The manuscript was created using R Markdown with integrated code and is available from the `power.transform` GitHub repository, together with intermediate analysis results for computationally intensive experiments.

- Materials availability: Not applicable
- Code availability: Location- and scale-invariant power transformations were implemented in the `power.transform` package for R, which is available from GitHub (<https://github.com/oncoray/power.transform>) and the CRAN repository (<https://cran.r-project.org/package=power.transform>). The manuscript was created using R Markdown with integrated code, and is available from the `power.transform` GitHub repository.
- Author contribution: Conceptualization: Alex Zwanenburg, Steffen Löck; Methodology: Alex Zwanenburg; Formal analysis and investigation: Alex Zwanenburg; Writing - original draft preparation: Alex Zwanenburg; Writing - review and editing: Alex Zwanenburg, Steffen Löck; Resources: Alex Zwanenburg, Steffen Löck; Supervision: Steffen Löck.

Appendix A Log-likelihood functions for location- and scale-invariant power transformation

Location- and scale-invariant Box-Cox and Yeo-Johnson transformations are parametrised using location x_0 and scale s parameters, in addition to transformation parameter λ . This leads to the following transformations. The location- and scale-invariant Box-Cox transformation is:

$$\phi_{BC}^{\lambda,x_0,s}(x_i) = \begin{cases} \left(\left(\frac{x_i - x_0}{s} \right)^\lambda - 1 \right) / \lambda & \text{if } \lambda \neq 0 \\ \log \left[\frac{x_i - x_0}{s} \right] & \text{if } \lambda = 0 \end{cases} \quad (A1)$$

where $x_i - x_0 > 0$. The location- and scale-invariant Yeo-Johnson transformation is:

$$\phi_{YJ}^{\lambda,x_0,s}(x_i) = \begin{cases} \left(\left(1 + \frac{x_i - x_0}{s} \right)^\lambda - 1 \right) / \lambda & \text{if } \lambda \neq 0 \text{ and } x_i - x_0 \geq 0 \\ \log \left[1 + \frac{x_i - x_0}{s} \right] & \text{if } \lambda = 0 \text{ and } x_i - x_0 \geq 0 \\ - \left(\left(1 - \frac{x_i - x_0}{s} \right)^{2-\lambda} - 1 \right) / (2 - \lambda) & \text{if } \lambda \neq 2 \text{ and } x_i - x_0 < 0 \\ - \log \left[1 - \frac{x_i - x_0}{s} \right] & \text{if } \lambda = 2 \text{ and } x_i - x_0 < 0 \end{cases} \quad (A2)$$

The parameters of these power transformations can be optimised by maximising the log-likelihood function, under the assumption that the transformed feature $\phi^{\lambda,x_0,s}(\mathbf{X})$ follows a normal distribution. The log-likelihood functions for conventional Box-Cox and Yeo-Johnson transformations are well-known. However, the introduction of scaling parameter s prevents their direct use. Here, we first derive the general form of the log-likelihood functions, and then derive their power-transformation specific definitions.

Let $f(x_1, \dots, x_n)$ be the probability density function of feature $\mathbf{X} = \{x_1, \dots, x_n\}$, and $f^{\lambda,x_0,s}(\phi^{\lambda,x_0,s}(x_1), \dots, \phi^{\lambda,x_0,s}(x_n))$ be the probability density function of the transformed feature $\phi^{\lambda,x_0,s}(\mathbf{X})$, that is assumed to follow a normal distribution.

The two probability density functions are related as follows:

$$f^{\lambda, x_0, s}(x_1, \dots, x_n) = f^{\lambda, x_0, s}(\phi^{\lambda, x_0, s}(x_1), \dots, \phi^{\lambda, x_0, s}(x_n)) |\mathbf{J}| \quad (\text{A3})$$

Where, $|\mathbf{J}|$ is the determinant of Jacobian \mathbf{J} . The Jacobian takes the following form, with off-diagonal elements 0:

$$\mathbf{J} = \begin{bmatrix} \frac{\partial}{\partial x_1} \phi^{\lambda, x_0, s}(x_1) & 0 & \dots & 0 \\ 0 & \frac{\partial}{\partial x_2} \phi^{\lambda, x_0, s}(x_2) & \dots & 0 \\ \vdots & \vdots & \ddots & \vdots \\ 0 & 0 & 0 & \frac{\partial}{\partial x_n} \phi^{\lambda, x_0, s}(x_n) \end{bmatrix} \quad (\text{A4})$$

Thus, $|\mathbf{J}| = \prod_{i=1}^n \frac{\partial}{\partial x_i} \phi^{\lambda, x_0, s}(x_i)$.

Since in our situation $\{x_1, \dots, x_n\}$ in $f^{\lambda, x_0, s}(x_1, \dots, x_n)$ are considered fixed (i.e., known), $f^{\lambda, x_0, s}(x_1, \dots, x_n)$ may be considered a likelihood function. The log-likelihood function $\mathcal{L}^{\lambda, x_0, s}$ is then:

$$\begin{aligned} \mathcal{L}^{\lambda, x_0, s} &= \log f^{\lambda, x_0, s}(x_1, \dots, x_n) \\ &= \log [f^{\lambda, x_0, s}(\phi^{\lambda, x_0, s}(x_1), \dots, \phi^{\lambda, x_0, s}(x_n))] + \log |\mathbf{J}| \\ &= \log [f^{\lambda, x_0, s}(\phi^{\lambda, x_0, s}(x_1), \dots, \phi^{\lambda, x_0, s}(x_n))] + \log \prod_{i=1}^n \frac{\partial}{\partial x_i} \phi^{\lambda, x_0, s}(x_i) \\ &= -\frac{n}{2} \log [2\pi\sigma^2] - \frac{1}{2\sigma^2} \sum_{i=1}^n (\phi^{\lambda, x_0, s}(x_i) - \mu)^2 + \sum_{i=1}^n \log \left[\frac{\partial}{\partial x_i} \phi^{\lambda, x_0, s}(x_i) \right] \end{aligned} \quad (\text{A5})$$

With μ the average of $\phi^{\lambda, x_0, s}(\mathbf{X})$ and σ^2 its variance. The first two terms derive directly from the log-likelihood function of a normal distribution, and are not specific to the type of power transformation used. However, the final term differs between Box-Cox and Yeo-Johnson transformations.

A.1 Location- and scale-invariant Box-Cox transformation

For the location- and scale-invariant Box-Cox transformation the partial derivative is:

$$\begin{aligned} \frac{\partial}{\partial x_i} \phi_{\text{BC}}^{\lambda, x_0, s}(x_i) &= \frac{1}{s} \left(\frac{x_i - x_0}{s} \right)^{\lambda-1} \\ &= \frac{1}{s^\lambda} (x_i - x_0)^{\lambda-1} \end{aligned} \quad (\text{A6})$$

Thus the final term in $\mathcal{L}_{\text{BC}}^{\lambda, x_0, s}$ is:

$$\begin{aligned}
\sum_{i=1}^n \log \frac{\partial}{\partial x_i} \phi_{BC}^{\lambda, x_0, s}(x_i) &= \sum_{i=1}^n \log [s^{-\lambda} (x_i - x_0)^{\lambda-1}] \\
&= \sum_{i=1}^n \log [s^{-\lambda}] + \log [(x_i - x_0)^{\lambda-1}] \\
&= -n\lambda \log s + (\lambda - 1) \sum_{i=1}^n \log [x_i - x_0]
\end{aligned} \tag{A7}$$

This leads to the following log-likelihood:

$$\begin{aligned}
\mathcal{L}_{BC}^{\lambda, x_0, s} &= -\frac{n}{2} \log [2\pi\sigma^2] - \frac{1}{2\sigma^2} \sum_{i=1}^n (\phi^{\lambda, x_0, s}(x_i) - \mu)^2 \\
&\quad - n\lambda \log s + (\lambda - 1) \sum_{i=1}^n \log [x_i - x_0]
\end{aligned} \tag{A8}$$

Similarly to [Raymaekers and Rousseeuw \(2024\)](#), sample weights w_i are introduced to facilitate robust power transformations. The weighted log-likelihood of the location- and scale-invariant Box-Cox transformation is:

$$\begin{aligned}
\mathcal{L}_{rBC}^{\lambda, x_0, s} &= -\frac{1}{2} \left(\sum_{i=1}^n w_i \right) \log [2\pi\sigma_w^2] - \frac{1}{2\sigma_w^2} \sum_{i=1}^n w_i (\phi^{\lambda, x_0, s}(x_i) - \mu_w)^2 \\
&\quad - \lambda \left(\sum_{i=1}^n w_i \right) \log s + (\lambda - 1) \sum_{i=1}^n w_i \log [x_i - x_0]
\end{aligned} \tag{A9}$$

where μ_w and σ_w^2 are the weighted mean and weighted variance of the Box-Cox transformed feature $\phi_{BC}^{\lambda, x_0, s}(\mathbf{X})$, respectively:

$$\sigma_w^2 = \frac{\sum_{i=1}^n w_i (\phi_{BC}^{\lambda, x_0, s}(x_i) - \mu_w)^2}{\sum_{i=1}^n w_i} \quad \text{with } \mu_w = \frac{\sum_{i=1}^n \phi_{BC}^{\lambda, x_0, s}(x_i)}{\sum_{i=1}^n w_i} \tag{A10}$$

A.2 Location- and scale-invariant Yeo-Johnson transformation

For the location- and scale-invariant Yeo-Johnson transformation, the partial derivative is:

$$\frac{\partial}{\partial x_i} \phi_{YJ}^{\lambda, x_0, s}(x_i) = \begin{cases} \frac{1}{s} \left(1 + \frac{x_i - x_0}{s}\right)^{\lambda-1} & \text{if } x_i - x_0 \geq 0 \\ \frac{1}{s} \left(1 - \frac{x_i - x_0}{s}\right)^{1-\lambda} & \text{if } x_i - x_0 < 0 \end{cases} \tag{A11}$$

Thus the final term in $\mathcal{L}_{\text{YJ}}^{\lambda, x_0, s}$ is:

$$\sum_{i=1}^n \log \frac{\partial}{\partial x_i} \phi_{\text{YJ}}^{\lambda, x_0, s}(x_i) = -n \log s + (\lambda - 1) \sum_{i=1}^n \operatorname{sgn}(x_i - x_0) \log \left[1 + \frac{|x_i - x_0|}{s} \right] \quad (\text{A12})$$

This leads to the following log-likelihood:

$$\begin{aligned} \mathcal{L}_{\text{YJ}}^{\lambda, x_0, s} = & -\frac{n}{2} \log [2\pi\sigma^2] - \frac{1}{2\sigma^2} \sum_{i=1}^n (\phi^{\lambda, x_0, s}(x_i) - \mu)^2 \\ & - n \log s + (\lambda - 1) \sum_{i=1}^n \operatorname{sgn}(x_i - x_0) \log \left[1 + \frac{|x_i - x_0|}{s} \right] \end{aligned} \quad (\text{A13})$$

The weighted log-likelihood for location- and scale-invariant Yeo-Johnson transformation is:

$$\begin{aligned} \mathcal{L}_{\text{rYJ}}^{\lambda, x_0, s} = & -\frac{1}{2} \left(\sum_{i=1}^n w_i \right) \log [2\pi\sigma_w^2] - \frac{1}{2\sigma_w^2} \sum_{i=1}^n w_i (\phi^{\lambda, x_0, s}(x_i) - \mu_w)^2 \\ & - \left(\sum_{i=1}^n w_i \right) \log s + (\lambda - 1) \sum_{i=1}^n w_i \operatorname{sgn}(x_i - x_0) \log \left[1 + \frac{|x_i - x_0|}{s} \right] \end{aligned} \quad (\text{A14})$$

where μ_w and σ_w^2 are the weighted mean and weighted variance of the Yeo-Johnson transformed feature $\phi_{\text{YJ}}^{\lambda, x_0, s}(\mathbf{X})$:

$$\sigma_w^2 = \frac{\sum_{i=1}^n w_i (\phi_{\text{YJ}}^{\lambda, x_0, s}(x_i) - \mu_w)^2}{\sum_{i=1}^n w_i} \quad \text{with } \mu_w = \frac{\sum_{i=1}^n \phi_{\text{YJ}}^{\lambda, x_0, s}(x_i)}{\sum_{i=1}^n w_i} \quad (\text{A15})$$

Appendix B Optimisation of transformation parameters

Maximum likelihood estimation (MLE) is commonly used to optimise parameters for power transformation. Generally, optimisation requires minimisation or maximisation of a criterion. In MLE, the maximised criterion is the log-likelihood function of the normal distribution. Here, we investigate power transformation using optimisation criteria that are closely related to test statistics for normality tests.

Let \mathbf{X} be a feature with ordered feature values, and $\mathbf{Y}^\lambda = \phi^\lambda(\mathbf{X})$ and $\mathbf{Y}^{\lambda, x_0, s} = \phi^{\lambda, x_0, s}(\mathbf{X})$ its transformed values using conventional and location- and scale-invariant power transformations, respectively. Since power transformations are monotonic, \mathbf{Y} will likewise be ordered.

Below we will focus on criteria based on the empirical density function and those based on skewness and kurtosis of the transformed feature. Other potential criteria, such as the Shapiro-Wilk test statistic ([Shapiro & Wilk, 1965](#)) are not investigated here. In the case of the Shapiro-Wilk test statistic this is because of lack of scalability to features with many (> 5000) instances, and because adapting the test statistic to include weights is not straightforward.

B.1 Empirical density function-based criteria

The first class of criteria is based on the empirical distribution function (EDF). Transformation parameters are then fit through minimisation of the distance between the empirical distribution function F_ϵ and the cumulative density function (CDF) of the normal distribution F_N . Let $F_\epsilon(x_i) = \frac{i-1/3}{n+1/3}$ be the empirical probability of instance i . The normal distribution is parametrised by location parameter μ and scale parameter σ , both of which have to be estimated from the data. For non-robust power transformations, μ and σ are sample mean and sample standard deviation, respectively. For robust power transformations, we estimate μ and σ as Huber M-estimates of location and scale of the transformed feature $\phi^{\lambda, x_0, s}(\mathbf{X})$ ([Huber, 1981](#)).

B.1.1 Anderson-Darling criterion

The Anderson-Darling criterion is based on the empirical distribution function of \mathbf{X} . We define this criterion as follows:

$$U_{AD}(\mathbf{X}, \lambda, x_0) = \frac{1}{\sum_{i=1}^n w_i} \sum_{i=1}^n w_i \frac{(F_\epsilon(x_i) - F_N(\phi^{\lambda, x_0, s}(x_i); \mu, \sigma))^2}{F_N(\phi^{\lambda, x_0, s}(x_i); \mu, \sigma)(1 - F_N(\phi^{\lambda, x_0, s}(x_i); \mu, \sigma))} \quad (\text{B16})$$

Here w_i are weights, and μ and σ are location and scale parameters. For non-robust power transformations, all $w_i = 1$. Note that this criterion is not the same as the Anderson-Darling test statistic ([Anderson & Darling, 1952](#)), which involves solving (or approximating) an integral function, contains an extra scalar multiplication term, and does not include weights. The Anderson-Darling criterion seeks to minimise the squared Euclidean distance between the EDF and the normal CDF, with differences at the upper and lower end of the normal CDF receiving more weight than those at the centre of the CDF.

B.1.2 Cramér-von Mises criterion

The Cramér-von Mises criterion is also based on the empirical distribution function of \mathbf{X} . We define the Cramér-von Mises criterion as follows:

$$U_{CvM}(\mathbf{X}, \lambda, x_0) = \frac{1}{\sum_{i=1}^n w_i} \sum_{i=1}^n w_i (F_\epsilon(x_i) - F_N(\phi^{\lambda, x_0, s}(x_i); \mu, \sigma))^2 \quad (\text{B17})$$

Here w_i are weights, and μ and σ are location and scale parameters. For non-robust power transformations, all $w_i = 1$. The criterion is similar to the Cramér-von Mises test statistic (Cramér, 1928, von Mises (1928)), aside from an additive scalar value and the introduction of weights. This criterion, like the Anderson-Darling criterion, seeks to minimise the squared Euclidean distance between the EDF and the normal CDF. Unlike the Anderson-Darling criterion, this criterion weights all instances equally.

For conventional power transformations with a fixed shift parameter, the transformation $\phi^{\lambda,x_0,s}(\mathbf{X})$ may be substituted by $\phi^\lambda(\mathbf{X})$ in the definition of the Cramér-von Mises criterion.

B.2 Skewness-kurtosis-based criteria

The second class of criteria seeks to reduce skewness and (excess) kurtosis of the transformed feature \mathbf{Y} . We will first define the location μ and scale σ of the transformed feature as these are required for computing skewness and kurtosis. Here, μ is defined as:

$$\mu = \frac{\sum_{i=1}^n \phi^{\lambda,x_0,s}(x_i)}{\sum_{i=1}^n w_i} \quad (\text{B18})$$

The location, or mean, is weighted by w_i , which equals 1 for non-robust transformations.

Then, σ^2 is defined as:

$$\sigma^2 = \frac{\sum_{i=1}^n w_i (\phi^{\lambda,x_0,s}(x_i) - \mu)^2}{\sum_{i=1}^n w_i} \quad (\text{B19})$$

Skewness is defined as:

$$s = \frac{\sum_{i=1}^n w_i (\phi^{\lambda,x_0,s}(x_i) - \mu)^3}{\sigma^3 \sum_{i=1}^n w_i} \quad (\text{B20})$$

Kurtosis is defined as:

$$k = \frac{\sum_{i=1}^n w_i (\phi^{\lambda,x_0,s}(x_i) - \mu)^4}{\sigma^4 \sum_{i=1}^n w_i} \quad (\text{B21})$$

B.2.1 D'Agostino criterion

The D'Agostino criterion defined here follows the D'Agostino K^2 test statistic (D'Agostino & Belanger, 1990). This test statistic is composed of two separate test statistics, one of which is related to skewness, and the other to kurtosis. Both test statistics are computed in several steps. Let us first define $\nu = \sum_{i=1}^n w_i$. Thus for non-robust power transformations, $\nu = n$.

For the skewness test statistic we first compute (D'Agostino & Belanger, 1990):

$$\beta_1 = s \sqrt{\frac{(\nu + 1)(\nu + 3)}{6(\nu - 2)}} \quad (\text{B22})$$

$$\beta_2 = 3 \frac{(\nu^2 + 27\nu - 70)(\nu + 1)(\nu + 3)}{(\nu - 2)(\nu + 5)(\nu + 7)(\nu + 9)} \quad (\text{B23})$$

$$\alpha = \sqrt{\frac{2}{\sqrt{2\beta_2} - 2}} \quad (\text{B24})$$

$$\delta = \frac{1}{\sqrt{\log \left[\sqrt{-1 + \sqrt{2 * \beta_2 - 2}} \right]}} \quad (\text{B25})$$

The skewness test statistic is then:

$$Z_s = \delta \log \left[\frac{\beta_1}{\alpha} + \sqrt{\frac{\beta_1^2}{\alpha^2} + 1} \right] \quad (\text{B26})$$

For the kurtosis test statistic we first compute ([Anscombe & Glynn, 1983](#); [D'Agostino & Belanger, 1990](#)):

$$\beta_1 = 3 \frac{\nu - 1}{\nu + 1} \quad (\text{B27})$$

$$\beta_2 = 24\nu \frac{(\nu - 2)(\nu - 3)}{(\nu + 1)^2(\nu + 3)(\nu + 5)} \quad (\text{B28})$$

$$\beta_3 = 6 \frac{\nu^2 - 5\nu + 2}{(\nu + 7)(\nu + 9)} \sqrt{6 \frac{(\nu + 3)(\nu + 5)}{\nu(\nu - 2)(\nu - 3)}} \quad (\text{B29})$$

$$\alpha_1 = 6 + \frac{8}{\beta_3} \left[\frac{2}{\beta_3} + \sqrt{1 + \frac{4}{\beta_3^2}} \right] \quad (\text{B30})$$

$$\alpha_2 = \frac{k - \beta_1}{\sqrt{\beta_2}} \quad (\text{B31})$$

The kurtosis test statistic is then:

$$Z_k = \sqrt{\frac{9\alpha_1}{2}} \left[1 - \frac{2}{9\alpha_1} - \left(\frac{1 - 2/\alpha_1}{1 + \alpha_2 \sqrt{2/(\alpha_1 - 4)}} \right)^{1/3} \right] \quad (\text{B32})$$

The D'Agostino K^2 test statistic and our criterion are the same, and are defined as:

$$U_{\text{DA}}(\mathbf{X}, \lambda, x_0) = Z_s^2 + Z_k^2 \quad (\text{B33})$$

The main difference between the test statistic as originally formulated, and the criterion proposed here is the presence of weights for robust power transformation.

B.2.2 Jarque-Bera criterion

The second criterion based on skewness and kurtosis is the Jarque-Bera criterion. It is relatively simple to compute compared to the D'Agostino criterion:

$$U_{JB}(\mathbf{X}, \lambda, x_0) = s^2 + (k - 3)^2 / 4 \quad (\text{B34})$$

The main difference between the above criterion and the Jarque-Bera test statistic (Jarque & Bera, 1980) is that a scalar multiplication is absent.

B.3 Optimisation using non-MLE criteria

Each of the above criteria can be used for optimisation, i.e.:

$$\left\{ \hat{\lambda}, \hat{x}_0, \hat{s}_0 \right\} = \underset{\lambda, x_0, s}{\operatorname{argmin}} U(\mathbf{X}, \lambda, x_0, s) \quad (\text{B35})$$

For conventional power transformations with fixed location and scale parameters, the transformation $\phi^{\lambda, x_0, s}(\mathbf{X})$ may be substituted by $\phi^\lambda(\mathbf{X})$, or equivalently, x_0 and s may be fixed:

$$\left\{ \hat{\lambda} \right\} = \underset{\lambda}{\operatorname{argmin}} U(\mathbf{X}, \lambda; x_0, s) \quad (\text{B36})$$

B.4 Simulations with other optimisation criteria

Invariance of location- and scale-invariant power transformations was assessed using the optimisation criteria in Appendix B. This follows the simulation in the main manuscript, where MLE was used for optimization. In short, we first randomly drew 10000 values from a normal distribution: $\mathbf{X}_{\text{normal}} = \{x_1, x_2, \dots, x_{10000}\} \sim \mathcal{N}(0, 1)$, or equivalently $\mathbf{X}_{\text{normal}} = \{x_1, x_2, \dots, x_{10000}\} \sim \mathcal{AGN}(0, 1/\sqrt{2}, 0.5, 2)$. The second distribution was a right-skewed normal distribution $\mathbf{X}_{\text{right}} = \{x_1, x_2, \dots, x_{10000}\} \sim \mathcal{AGN}(0, 1/\sqrt{2}, 0.2, 2)$. The third distribution was a left-skewed normal distribution $\mathbf{X}_{\text{left}} = \{x_1, x_2, \dots, x_{10000}\} \sim \mathcal{AGN}(0, 1/\sqrt{2}, 0.8, 2)$.

We then computed transformation parameter λ using the original definitions (equations 1 and 2) and the location- and scale-invariant definitions (equations 3 and 4) for each distribution using different optimisation criteria. To assess location invariance, a positive value d_{shift} was added to each distribution with $d_{\text{shift}} \in [1, 10^6]$. Similarly, to assess scale invariance, each distribution was multiplied by a positive value d_{scale} , where $d_{\text{scale}} \in [1, 10^6]$.

The results are shown in Figure B1.

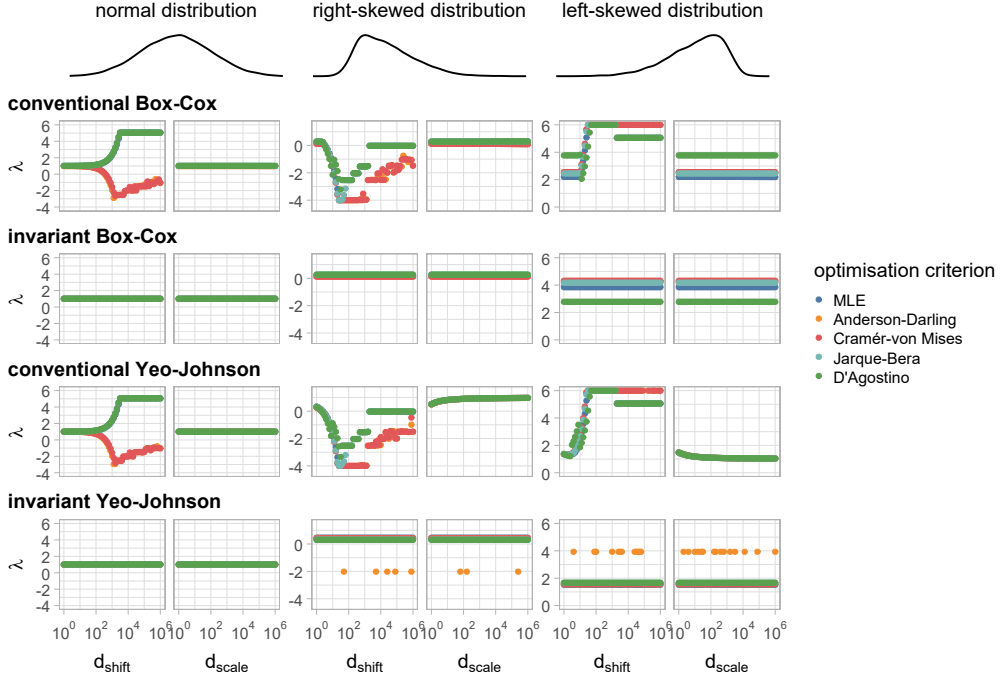


Fig. B1 Invariant power transformation produces transformation parameters that are invariant to location and scale. Samples were drawn from normal, right-skewed and left-skewed distributions, respectively, which then underwent a shift d_{shift} or multiplication by d_{scale} . Estimates of the transformation parameter λ for the conventional power transformations show strong dependency on the overall location and scale of the distribution and the optimisation criterion, whereas estimates obtained for the location- and scale-invariant power transformations are constant. For location- and scale-invariant power transformations, the Anderson-Darling criterion leads to unstable estimates of λ for skewed distributions, possibly due to large weights being assigned to samples at the upper and lower ends of the distribution.

Appendix C Empirical central normality test critical values

Critical values for the empirical central normality test at $\kappa = 0.80$ are found in Table C1.

Table C1 Critical values of test statistic $\tau_{\alpha,n,\kappa=0.80}$ for central normality at $\kappa = 0.80$, as a function of significance level α and number of instances n . The values in this table should be divided by 100 before use.

$n \setminus \alpha$	0.001	0.01	0.025	0.05	0.1	0.2	0.5	0.8	0.9
5	200.88	90.25	64.46	49.04	36.07	27.70	19.28	13.41	10.90
10	45.90	31.78	27.12	24.14	21.23	18.30	13.68	10.20	8.71
20	28.88	22.53	19.96	18.01	15.99	13.93	10.67	8.26	7.27
50	16.86	14.10	12.66	11.55	10.28	8.95	7.00	5.53	4.91
100	12.41	10.00	9.02	8.21	7.36	6.45	5.02	4.00	3.58
200	8.65	7.05	6.37	5.80	5.22	4.57	3.57	2.84	2.54
500	5.54	4.47	4.03	3.69	3.30	2.90	2.27	1.81	1.63
1000	3.88	3.17	2.86	2.60	2.34	2.05	1.61	1.28	1.15
2000	2.79	2.24	2.03	1.84	1.66	1.45	1.14	0.91	0.82
5000	1.75	1.41	1.27	1.17	1.05	0.92	0.72	0.58	0.52
10000	1.21	1.00	0.90	0.82	0.74	0.65	0.51	0.41	0.36

Appendix D Assessing transformations using simulated data

D.1 Ranking Box-Cox transformations

Box-Cox transformations were assessed in the same manner as Yeo-Johnson transformations. The results are shown in Table D2.

Table D2 Comparison of average rank between Box-Cox transformation methods based on either residual error (without outliers) or residual error of the central portion (with outliers; $\kappa = 0.80$) over 3 datasets with 100000 sequences each. The clean dataset consists of sequences derived through inverse Box-Cox transformation of data sampled from a standard normal distribution. The dirty dataset contains sequences sampled from asymmetric generalised normal distributions. The shifted dataset also contains sequences sampled from asymmetric generalised normal distributions, but centred at 100, and scaled by 0.001. If necessary, each sequence was shifted so that every element had a strictly positive value. Several transformation methods include normalisation before transformation, indicated by z-score normalisation (norm.) or robust scaling. A rank of 1 is the best and a rank of 9 the worst. For each dataset, the best ranking transformation is marked in bold.

transformation	dataset: outliers:	clean		dirty		shifted	
		no	yes	no	yes	no	yes
none		7.63	6.95	7.29	6.59	7.47	6.78
conventional		3.11	5.98	5.41	6.18	6.51	6.10
conventional (z-score norm.)		4.15	6.27	4.83	6.32	4.34	5.84
conventional (robust scaling)		4.20	6.29	4.84	6.31	4.35	5.84
Raymaekers-Rousseeuw		4.50	3.56	5.39	3.69	6.30	5.80
Raymaekers-Rousseeuw (z-score norm.)		6.23	3.80	4.93	3.85	4.48	3.50
Raymaekers-Rousseeuw (robust scaling)		6.12	3.80	4.99	3.87	4.53	3.51
invariant		2.96	5.59	3.62	6.01	3.51	5.58
robust invariant		6.10	2.76	3.68	2.19	3.51	2.00

D.2 Ranking Yeo-Johnson transformations: residual errors

In the main manuscript, transformation methods are compared by ranking within each experiment, defined by the combination of sequence and absence/presence of outliers. This allows for direct comparison of methods between different experiments.

Table D3 shows the average normalised residual error for these transformation methods. This metric is computed from the residual error and the residual error of the central portion ($\kappa = 0.80$) for sequences without and with outliers, respectively. In each experiment, the respective residual error was normalised by dividing with the sequence length, and can be interpreted as the average residual error of a single sample. This reduces the effect of sequence length on the residual error.

Table D4 shows the average normalised difference in residual error between the best method for each experiment and the individual methods. As above, normalisation was done by division by the length of the sequence corresponding to each experiment.

Both tables show that the differences between best-performing methods on each dataset are relatively small.

Table D3 Comparison of average normalised residual error between Yeo-Johnson transformation methods based on either the residual error (without outliers) or the residual error of the central portion (with outliers; $\kappa = 0.80$) over 3 datasets with 100000 sequences each. Residual errors were normalised by sequence length to reduce the effect of sequence length on the residual error. The clean dataset consists of sequences derived through inverse Yeo-Johnson transformation of data sampled from a standard normal distribution. The dirty dataset contains sequences sampled from asymmetric generalised normal distributions, centred at 0. The shifted dataset also contains sequences sampled from asymmetric generalised normal distributions, but centred at 100, and scaled by 0.001. Several transformation methods include normalisation before transformation, indicated by z-score normalisation (norm.) or robust scaling. A lower normalised residual error is better. Discrepancies with the rank-based method may occur, as even with normalisation residual errors are not fully comparable between experiments, whereas the ranks achieved within each experiment are.

transformation	dataset: outliers:	clean		dirty		shifted	
		no	yes	no	yes	no	yes
none		0.202	0.112	0.128	0.080	0.129	0.080
conventional		0.058	0.094	0.085	0.078	0.129	0.080
conventional (z-score norm.)		0.061	0.094	0.091	0.073	0.091	0.073
conventional (robust scaling)		0.058	0.094	0.090	0.073	0.090	0.073
Raymaekers-Rousseeuw		0.071	0.055	0.092	0.279	0.129	0.080
Raymaekers-Rousseeuw (z-score norm.)		0.087	0.057	0.097	0.060	0.097	0.060
Raymaekers-Rousseeuw (robust scaling)		0.071	0.056	0.095	0.059	0.095	0.059
invariant		0.057	0.099	0.083	0.075	0.083	0.075
robust invariant		0.069	0.066	0.084	0.058	0.084	0.058

Table D4 Comparison of average difference in residual error between Yeo-Johnson transformation methods and the best transformation method within each experiment, normalised by the corresponding sequence length. This is based on either the residual error (without outliers) or the residual error of the central portion (with outliers; $\kappa = 0.80$) over 3 datasets with 100000 sequences each. Residual errors were normalised by sequence length to reduce the effect of sequence length on the residual error. The clean dataset consists of sequences derived through inverse Yeo-Johnson transformation of data sampled from a standard normal distribution. The dirty dataset contains sequences sampled from asymmetric generalised normal distributions, centred at 0. The shifted dataset also contains sequences sampled from asymmetric generalised normal distributions, but centred at 100, and scaled by 0.001. Several transformation methods include normalisation before transformation, indicated by z-score normalisation (norm.) or robust scaling. A lower difference is better, with a minimum value of 0.0. Discrepancies with the rank-based method may occur, as normalised differences in residual error are not fully comparable between experiments, whereas the ranks achieved within each experiment are.

transformation	dataset: outliers:	clean		dirty		shifted	
		no	yes	no	yes	no	yes
none		0.150	0.068	0.050	0.033	0.049	0.033
conventional		0.005	0.049	0.006	0.032	0.049	0.033
conventional (z-score norm.)		0.008	0.049	0.013	0.026	0.011	0.025
conventional (robust scaling)		0.005	0.050	0.012	0.026	0.010	0.026
Raymaekers-Rousseeuw		0.018	0.011	0.014	0.233	0.049	0.033
Raymaekers-Rousseeuw (z-score norm.)		0.034	0.012	0.018	0.014	0.017	0.013
Raymaekers-Rousseeuw (robust scaling)		0.018	0.011	0.017	0.012	0.015	0.011
invariant		0.004	0.054	0.005	0.029	0.003	0.028
robust invariant		0.016	0.021	0.006	0.011	0.004	0.010

D.3 Ranking Yeo-Johnson transformations: effect of sequence length

The main manuscript shows the overall ranking of different Yeo-Johnson-based power transformation methods across three sets of problems. To assess the effect of limited sequence lengths, we perform ranking on subsets of the experiment. The results for ranking the subset of sequences with 30 samples or fewer ($n = 16001$) is shown in Table D5. In the clean dataset without outliers, where all sequences were sampled from a normal distribution and then underwent an inverse Yeo-Johnson transformation, conventional and location- and scale-invariant are ranked similarly, with no clear advantage to any method. For the remaining datasets, the robust location- and scale-invariant method ranked best. It slightly outperformed (robustly scaled) conventional Yeo-Johnson transformations and (z-score normalised) robust transformations (Raymaekers & Rousseeuw, 2024), in datasets without and with outliers, respectively.

In the subset for larger sequence lengths, with at least 1000 samples per sequence ($n = 33037$), the cost of making the location- and scale-invariant transformation robust against outliers becomes more apparent (Table D7). In the clean dataset without outliers, down-weighting of the tails of the distribution by the robust location- and scale-invariant method leads to larger residuals compared to other methods (Table D8).

Table D5 Comparison of average rank between Yeo-Johnson transformation methods based on either residual error (without outliers) or residual error of the central portion (with outliers; $\kappa = 0.80$) over 3 datasets with 16001 sequences each. Each sequence contained 30 samples or fewer. The clean dataset consists of sequences derived through inverse Yeo-Johnson transformation of data sampled from a standard normal distribution. The dirty dataset contains sequences sampled from asymmetric generalised normal distributions, centred at 0. The shifted dataset also contains sequences sampled from asymmetric generalised normal distributions, but centred at 100, and scaled by 0.001. Several transformation methods include normalisation before transformation, indicated by z-score normalisation (norm.) or robust scaling. A rank of 1 is the best and a rank of 9 the worst. For each dataset, the best ranking transformation is marked in bold.

transformation	dataset: outliers:	clean		dirty		shifted	
		no	yes	no	yes	no	yes
none		7.75	6.81	7.27	6.40	7.45	6.60
conventional		4.19	5.47	4.48	5.78	6.55	5.94
conventional (z-score norm.)		4.36	5.12	5.01	4.99	4.35	4.70
conventional (robust scaling)		4.05	5.63	4.38	5.49	3.76	5.20
Raymaekers-Rousseeuw		5.36	4.19	5.14	4.62	6.32	5.83
Raymaekers-Rousseeuw (z-score norm.)		5.56	4.08	5.67	4.05	5.03	3.81
Raymaekers-Rousseeuw (robust scaling)		5.33	4.14	5.15	4.15	4.55	3.94
invariant		4.11	5.92	4.12	5.67	3.62	5.37
robust invariant		4.28	3.65	3.79	3.85	3.37	3.61

Table D6 Comparison of average normalised residual error between Yeo-Johnson transformation methods based on either the residual error (without outliers) or the residual error of the central portion (with outliers; $\kappa = 0.80$) over 3 datasets with 16001 sequences each. Residual errors were normalised by sequence length to reduce the effect of sequence length on the residual error. Each sequence contained 30 samples or fewer. The clean dataset consists of sequences derived through inverse Yeo-Johnson transformation of data sampled from a standard normal distribution. The dirty dataset contains sequences sampled from asymmetric generalised normal distributions, centred at 0. The shifted dataset also contains sequences sampled from asymmetric generalised normal distributions, but centred at 100, and scaled by 0.001. Several transformation methods include normalisation before transformation, indicated by z-score normalisation (norm.) or robust scaling. A lower normalised residual error is better. Discrepancies with the rank-based method may occur, as even with normalisation residual errors are not fully comparable between experiments, whereas the ranks achieved within each experiment are.

transformation	dataset: outliers:	clean		dirty		shifted	
		no	yes	no	yes	no	yes
none		0.246	0.173	0.186	0.156	0.187	0.157
conventional		0.139	0.142	0.142	0.132	0.187	0.157
conventional (z-score norm.)		0.139	0.142	0.142	0.130	0.142	0.130
conventional (robust scaling)		0.139	0.142	0.141	0.130	0.141	0.130
Raymaekers-Rousseeuw		0.211	0.151	0.183	1.515	0.187	0.157
Raymaekers-Rousseeuw (z-score norm.)		0.295	0.161	0.175	0.156	0.175	0.156
Raymaekers-Rousseeuw (robust scaling)		0.209	0.155	0.172	0.144	0.172	0.144
invariant		0.141	0.144	0.140	0.132	0.140	0.132
robust invariant		0.141	0.125	0.140	0.119	0.140	0.119

Table D7 Comparison of average rank between Yeo-Johnson transformation methods based on either residual error (without outliers) or residual error of the central portion (with outliers; $\kappa = 0.80$) over 3 datasets with 33037 sequences each. Each sequence contained between 1000 and 10000 samples. The clean dataset consists of sequences derived through inverse Yeo-Johnson transformation of data sampled from a standard normal distribution. The dirty dataset contains sequences sampled from asymmetric generalised normal distributions, centred at 0. The shifted dataset also contains sequences sampled from asymmetric generalised normal distributions, but centred at 100, and scaled by 0.001. Several transformation methods include normalisation before transformation, indicated by z-score normalisation (norm.) or robust scaling. A rank of 1 is the best and a rank of 9 the worst. For each dataset, the best ranking transformation is marked in bold.

transformation	dataset: outliers:	clean		dirty		shifted	
		no	yes	no	yes	no	yes
none		8.85	8.14	7.35	6.29	7.41	6.87
conventional		3.50	5.65	3.52	7.78	6.42	6.05
conventional (z-score norm.)		5.24	5.94	7.34	4.98	6.26	4.79
conventional (robust scaling)		3.53	6.98	5.97	5.79	4.87	5.65
Raymaekers-Rousseeuw		4.15	2.81	3.37	3.72	6.19	5.79
Raymaekers-Rousseeuw (z-score norm.)		5.34	1.86	6.57	3.39	5.49	3.30
Raymaekers-Rousseeuw (robust scaling)		4.20	2.33	5.21	3.36	4.12	3.23
invariant		2.36	7.59	2.66	6.82	1.98	6.81
robust invariant		7.83	3.70	3.01	2.88	2.26	2.51

Table D8 Comparison of average normalised residual error between Yeo-Johnson transformation methods based on either the residual error (without outliers) or the residual error of the central portion (with outliers; $\kappa = 0.80$) over 3 datasets with 16001 sequences each. Residual errors were normalised by sequence length to reduce the effect of sequence length on the residual error. Each sequence contained between 1000 and 10000 samples. The clean dataset consists of sequences derived through inverse Yeo-Johnson transformation of data sampled from a standard normal distribution. The dirty dataset contains sequences sampled from asymmetric generalised normal distributions, centred at 0. The shifted dataset also contains sequences sampled from asymmetric generalised normal distributions, but centred at 100, and scaled by 0.001. Several transformation methods include normalisation before transformation, indicated by z-score normalisation (norm.) or robust scaling. A lower normalised residual error is better. Discrepancies with the rank-based method may occur, as even with normalisation residual errors are not fully comparable between experiments, whereas the ranks achieved within each experiment are.

transformation	dataset: outliers:	clean		dirty		shifted	
		no	yes	no	yes	no	yes
none		0.186	0.091	0.106	0.053	0.106	0.053
conventional		0.014	0.076	0.060	0.057	0.106	0.053
conventional (z-score norm.)		0.021	0.076	0.070	0.050	0.070	0.050
conventional (robust scaling)		0.014	0.076	0.069	0.050	0.069	0.050
Raymaekers-Rousseeuw		0.015	0.021	0.060	0.030	0.106	0.053
Raymaekers-Rousseeuw (z-score norm.)		0.021	0.020	0.070	0.030	0.070	0.030
Raymaekers-Rousseeuw (robust scaling)		0.015	0.020	0.068	0.030	0.068	0.030
invariant		0.013	0.084	0.059	0.055	0.059	0.055
robust invariant		0.034	0.042	0.061	0.032	0.061	0.032

D.4 Examples using clean data

Robust transformations are hypothesised to have a cost in efficiency for data without outliers, i.e. clean data. Here we draw nine sequences with elements randomly drawn from a standard normal distribution $\mathcal{N}(0, 1)$. Subsequently, we perform an inverse transformation $(\phi^{\lambda, 0, 1})^{-1}$, with $\lambda \in (0, 2)$.

The sequences drawn resulted from the permutations of the number of elements of each sequence ($n \in \{30, 100, 500\}$) and transformation parameter for the inverse transformation $\lambda \in \{0.1, 1.0, 1.9\}$. Each sequence then underwent power transformation using Box-Cox and Yeo-Johnson transformations. For Box-Cox transformations, each sequence was shifted prior to inverse transformation ensuring all elements were strictly positive after inverse transformation.

Results for Box-Cox transformations are shown in Table D12, D13, and D14. Additionally, results for Yeo-Johnson transformations are shown in Table D9, D10, and D11. As may be observed, in these examples robust location- and shift-invariant transformations have higher residual errors because of low weights being assigned to tails of a distribution. This is also shown in Tables 3 and D2 for clean data without outliers.

Table D9 Residual errors for features from simulated clean data without outliers after Yeo-Johnson transformation to normality. Several transformation methods include normalisation before transformation, indicated by z-score normalisation (norm.) or robust scaling.

transformation	$\lambda:$	n: 30			100			500		
		0.1	1.0	1.9	0.1	1.0	1.9	0.1	1.0	1.9
none		4.0	3.4	4.6	40.1	8.9	20.8	184.6	10.1	191.8
conventional		2.7	3.3	3.6	6.5	8.1	5.6	14.2	10.1	16.1
conventional (z-score norm.)		2.5	3.3	3.7	9.8	8.1	5.6	24.1	10.1	15.9
conventional (robust scaling)		2.6	3.3	3.7	7.4	8.2	5.6	15.5	10.1	14.0
Raymaekers-Rousseeuw		3.8	3.3	3.6	6.5	8.5	5.6	14.4	11.0	17.6
Raymaekers-Rousseeuw (z-score norm.)		2.6	3.3	3.7	9.8	8.5	5.6	24.1	11.1	15.9
Raymaekers-Rousseeuw (robust scaling)		2.6	3.3	3.7	7.4	8.6	5.6	15.4	11.1	15.1
invariant		3.0	3.5	3.6	5.0	8.1	5.6	13.1	10.9	17.8
robust invariant		3.0	3.4	3.6	5.5	10.1	6.2	18.7	13.2	32.8

Table D10 Transformation parameter λ for features from simulated clean data without outliers after Yeo-Johnson transformation to normality. Several transformation methods include normalisation before transformation, indicated by z-score normalisation (norm.) or robust scaling.

transformation	n:	30			100			500		
	$\lambda:$	0.1	1.0	1.9	0.1	1.0	1.9	0.1	1.0	1.9
conventional		0.6	1.2	1.5	0.0	0.9	1.6	0.1	1.0	1.9
conventional (z-score norm.)		0.5	1.2	1.5	-0.2	0.9	1.7	-0.2	1.0	2.2
conventional (robust scaling)		0.5	1.3	1.6	-0.3	0.9	1.7	-0.2	1.0	2.1
Raymaekers-Rousseeuw		1.0	1.2	1.5	0.0	0.7	1.6	0.1	1.0	1.9
Raymaekers-Rousseeuw (z-score norm.)		0.7	1.2	1.5	-0.2	0.7	1.7	-0.2	1.0	2.2
Raymaekers-Rousseeuw (robust scaling)		0.6	1.3	1.6	-0.3	0.6	1.7	-0.2	1.0	2.1
invariant		0.4	1.4	1.7	0.1	0.9	1.8	0.1	1.1	3.0
robust invariant		0.5	1.1	1.5	-0.1	0.7	1.7	0.1	1.1	1.9

Table D11 p-values of empirical central normality tests ($\kappa = 0.80$) for features from simulated clean data without outliers after Yeo-Johnson transformation to normality. Several transformation methods include normalisation before transformation, indicated by z-score normalisation (norm.) or robust scaling.

transformation	n:	30			100			500		
	$\lambda:$	0.1	1.0	1.9	0.1	1.0	1.9	0.1	1.0	1.9
none		0.968	0.742	0.450	< 0.001	0.058	0.004	< 0.001	0.963	< 0.001
conventional		0.966	0.494	0.498	0.632	0.145	0.707	0.828	0.986	0.358
conventional (z-score norm.)		0.955	0.471	0.529	0.169	0.147	0.853	0.260	0.986	0.603
conventional (robust scaling)		0.957	0.470	0.523	0.674	0.146	0.775	0.828	0.986	0.347
Raymaekers-Rousseeuw		0.972	0.494	0.498	0.632	0.518	0.707	0.785	0.939	0.609
Raymaekers-Rousseeuw (z-score norm.)		0.974	0.471	0.529	0.169	0.519	0.853	0.289	0.935	0.568
Raymaekers-Rousseeuw (robust scaling)		0.968	0.470	0.523	0.674	0.536	0.775	0.762	0.935	0.609
invariant		0.978	0.353	0.448	0.701	0.161	0.588	0.872	0.984	0.667
robust invariant		0.985	0.660	0.556	0.871	0.652	0.525	0.888	0.968	0.411

Table D12 Residual errors for features from simulated clean data without outliers after Box-Cox transformation to normality. Several transformation methods include normalisation before transformation, indicated by z-score normalisation (norm.) or robust scaling.

transformation	n:	30			100			500		
	λ :	0.1	1.0	1.9	0.1	1.0	1.9	0.1	1.0	1.9
none		5.3	3.4	3.8	45.7	8.9	6.0	221.8	10.1	29.7
conventional		2.4	3.2	3.5	5.9	8.4	5.5	14.3	9.8	16.1
conventional (z-score norm.)		2.4	3.2	3.7	5.4	8.7	5.5	14.0	10.4	16.1
conventional (robust scaling)		2.4	3.2	3.7	5.4	8.7	5.5	14.0	10.4	16.1
Raymaekers-Rousseeuw		2.4	3.2	3.5	5.9	13.3	5.7	16.1	13.6	16.9
Raymaekers-Rousseeuw (z-score norm.)		2.4	3.2	4.9	6.3	8.9	6.2	19.1	19.0	19.9
Raymaekers-Rousseeuw (robust scaling)		2.4	3.2	4.9	6.3	8.9	6.2	18.4	19.0	19.9
invariant		2.4	3.2	3.7	5.4	8.7	5.5	13.7	9.9	16.0
robust invariant		2.4	4.3	4.7	8.9	20.4	6.7	14.1	15.8	37.6

Table D13 Transformation parameter λ for features from simulated clean data without outliers after Box-Cox transformation to normality. Several transformation methods include normalisation before transformation, indicated by z-score normalisation (norm.) or robust scaling.

transformation	n:	30			100			500		
	λ :	0.1	1.0	1.9	0.1	1.0	1.9	0.1	1.0	1.9
conventional		0.4	1.3	0.5	0.0	0.9	0.7	0.1	1.1	2.0
conventional (z-score norm.)		0.4	1.1	0.8	0.2	0.9	0.8	0.1	1.0	1.4
conventional (robust scaling)		0.4	1.1	0.8	0.2	0.9	0.8	0.1	1.0	1.4
Raymaekers-Rousseeuw		0.4	1.3	0.5	0.0	-0.1	0.5	0.1	0.9	1.8
Raymaekers-Rousseeuw (z-score norm.)		0.4	1.1	0.4	0.1	0.8	0.7	0.1	0.9	1.2
Raymaekers-Rousseeuw (robust scaling)		0.4	1.1	0.4	0.1	0.8	0.7	0.1	0.9	1.2
invariant		0.4	1.6	0.8	0.2	0.9	0.8	0.1	1.1	1.9
robust invariant		0.5	0.8	0.4	0.0	0.2	0.7	0.1	0.9	0.9

Table D14 p-values of empirical central normality tests ($\kappa = 0.80$) for features from simulated clean data without outliers after Box-Cox transformation to normality. Several transformation methods include normalisation before transformation, indicated by z-score normalisation (norm.) or robust scaling.

transformation	n: $\lambda:$	30			100			500		
		0.1	1.0	1.9	0.1	1.0	1.9	0.1	1.0	1.9
none		0.911	0.742	0.365	< 0.001	0.057	0.623	< 0.001	0.962	0.789
conventional		0.922	0.590	0.482	0.726	0.100	0.718	0.794	0.984	0.380
conventional (z-score norm.)		0.920	0.690	0.506	0.505	0.114	0.714	0.888	0.957	0.594
conventional (robust scaling)		0.920	0.690	0.506	0.504	0.114	0.714	0.887	0.957	0.594
Raymaekers-Rousseeuw		0.922	0.590	0.482	0.726	0.689	0.736	0.582	0.869	0.531
Raymaekers-Rousseeuw (z-score norm.)		0.920	0.690	0.660	0.876	0.172	0.710	0.521	0.670	0.774
Raymaekers-Rousseeuw (robust scaling)		0.920	0.690	0.660	0.876	0.172	0.710	0.568	0.670	0.774
invariant		0.921	0.549	0.506	0.505	0.114	0.715	0.853	0.986	0.387
robust invariant		0.954	0.752	0.656	0.956	0.699	0.698	0.852	0.801	0.623

Appendix E Experimental results

The effect of using location- and scale-invariant transformations was investigated using real-world datasets, as described in the main manuscript.

E.1 Yeo-Johnson transformation

Additional results for Yeo-Johnson transformations are shown in Tables [E15](#), [E16](#), [E17](#).

Table E15 Residual errors for features from real-world datasets after Yeo-Johnson transformation to normality. Several transformation methods include normalisation before transformation, indicated by z-score normalisation (norm.) or robust scaling. AWT: arterial wall thickness; FE: fuel efficiency; PBM: penguin body mass

feature	age	AWT	FE	latitude	PBM
none	16.5	110.1	54.5	328.4	48.0
conventional	11.5	30.0	55.3	319.0	32.2
conventional (z-score norm.)	11.5	19.3	49.0	326.2	33.3
conventional (robust scaling)	11.3	33.3	55.9	326.5	31.5
Raymaekers-Rousseeuw	11.5	136.7	47.7	315.1	32.2
Raymaekers-Rousseeuw (z-score norm.)	13.2	214.5	57.4	326.2	33.3
Raymaekers-Rousseeuw (robust scaling)	13.4	202.9	56.9	326.4	31.5
invariant	8.8	12.2	44.0	326.4	26.8
robust invariant	9.3	30.2	55.8	308.1	22.0

Table E16 Transformation parameter λ for features from real-world datasets after Yeo-Johnson transformation to normality. Several transformation methods include normalisation before transformation, indicated by z-score normalisation (norm.) or robust scaling. AWT: arterial wall thickness; FE: fuel efficiency; PBM: penguin body mass

feature	age	AWT	FE	latitude	PBM
conventional	2.0	-0.7	-0.1	62.1	-0.5
conventional (z-score norm.)	1.2	-1.7	-0.1	1.3	0.6
conventional (robust scaling)	1.2	0.0	0.3	1.3	0.6
Raymaekers-Rousseeuw	2.0	1.1	0.8	95.4	-0.5
Raymaekers-Rousseeuw (z-score norm.)	1.3	1.4	1.0	1.3	0.6
Raymaekers-Rousseeuw (robust scaling)	1.3	1.2	1.0	1.3	0.6
invariant	1.3	0.2	-1.3	1.5	0.5
robust invariant	1.3	-0.3	1.0	1.1	0.3

Table E17 p-values of empirical central normality tests ($\kappa = 0.80$) for features from real-world datasets after Yeo-Johnson transformation to normality. Several transformation methods include normalisation before transformation, indicated by z-score normalisation (norm.) or robust scaling. AWT: arterial wall thickness; FE: fuel efficiency; PBM: penguin body mass

feature	age	AWT	FE	latitude	PBM
none	0.541	0.731	0.546	< 0.001	< 0.001
conventional	0.919	< 0.001	< 0.001	< 0.001	0.032
conventional (z-score norm.)	0.845	0.007	< 0.001	< 0.001	0.031
conventional (robust scaling)	0.847	< 0.001	< 0.001	< 0.001	0.063
Raymaekers-Rousseeuw	0.919	0.802	0.205	< 0.001	0.032
Raymaekers-Rousseeuw (z-score norm.)	0.540	0.830	0.655	< 0.001	0.031
Raymaekers-Rousseeuw (robust scaling)	0.438	0.878	0.669	< 0.001	0.064
invariant	0.947	0.071	< 0.001	< 0.001	0.123
robust invariant	0.867	0.091	0.587	< 0.001	0.477

E.2 Box-Cox transformation

Results for Box-Cox transformations are shown in Tables E18, E19 and E20.

Table E18 Residual errors for features from real-world datasets after Box-Cox transformation to normality. Several transformation methods include normalisation before transformation, indicated by z-score normalisation (norm.) or robust scaling. AWT: arterial wall thickness; FE: fuel efficiency; PBM: penguin body mass

feature	age	AWT	FE	latitude	PBM
none	16.5	110.1	54.5	328.4	48.0
conventional	11.5	33.5	55.7	318.9	32.2
conventional (z-score norm.)	12.9	44.5	58.8	305.3	27.3
conventional (robust scaling)	12.9	44.7	59.0	305.3	27.3
Raymaekers-Rousseeuw	11.5	127.1	47.6	314.8	32.2
Raymaekers-Rousseeuw (z-score norm.)	13.1	54.8	127.5	510.2	23.6
Raymaekers-Rousseeuw (robust scaling)	13.1	100.2	44.9	423.2	23.6
invariant	11.6	28.0	48.4	311.8	27.3
robust invariant	12.8	150.1	60.5	646.0	27.4

Table E19 Transformation parameter λ for features from real-world datasets after Box-Cox transformation to normality. Several transformation methods include normalisation before transformation, indicated by z-score normalisation (norm.) or robust scaling. AWT: arterial wall thickness; FE: fuel efficiency; PBM: penguin body mass

feature	age	AWT	FE	latitude	PBM
conventional	1.9	-0.5	-0.1	62.1	-0.5
conventional (z-score norm.)	1.2	0.1	0.2	1.2	0.5
conventional (robust scaling)	1.2	0.1	0.1	1.2	0.5
Raymaekers-Rousseeuw	1.9	1.1	0.8	95.9	-0.5
Raymaekers-Rousseeuw (z-score norm.)	1.2	0.6	-0.5	0.6	0.3
Raymaekers-Rousseeuw (robust scaling)	1.2	1.0	0.8	0.7	0.3
invariant	1.7	-1.0	-0.7	1.9	0.5
robust invariant	1.3	1.2	1.1	0.4	0.1

Table E20 p-values of empirical central normality tests ($\kappa = 0.80$) for features from real-world datasets after Box-Cox transformation to normality. Several transformation methods include normalisation before transformation, indicated by z-score normalisation (norm.) or robust scaling. AWT: arterial wall thickness; FE: fuel efficiency; PBM: penguin body mass

feature	age	AWT	FE	latitude	PBM
none	0.541	0.731	0.546	< 0.001	< 0.001
conventional	0.919	< 0.001	< 0.001	< 0.001	0.032
conventional (z-score norm.)	0.815	0.001	< 0.001	< 0.001	0.057
conventional (robust scaling)	0.815	0.001	< 0.001	< 0.001	0.057
Raymaekers-Rousseeuw	0.919	0.787	0.200	< 0.001	0.032
Raymaekers-Rousseeuw (z-score norm.)	0.799	0.152	< 0.001	< 0.001	0.285
Raymaekers-Rousseeuw (robust scaling)	0.799	0.674	0.060	< 0.001	0.285
invariant	0.919	0.001	< 0.001	< 0.001	0.057
robust invariant	0.813	0.817	0.736	< 0.001	0.403

References

Alfons, A. (2021, November). robustHD: An R package for robust regression with high-dimensional data. *J. Open Source Softw.*, 6(67), 3786, <https://doi.org/10.21105/joss.03786>

Anderson, T.W., & Darling, D.A. (1952, June). Asymptotic theory of certain “goodness of fit” criteria based on stochastic processes. *Annals of Mathematical Statistics*, 23(2), 193–212, <https://doi.org/10.1214/aoms/1177729437>

Anscombe, F.J., & Glynn, W.J. (1983, April). Distribution of the kurtosis statistic b2 for normal samples. *Biometrika*, 70(1), 227–234, <https://doi.org/10.1093/biomet/70.1.227>

Bartlett, M.S. (1947, March). The use of transformations. *Biometrics*, 3(1), 39–52, <https://doi.org/10.2307/3001536>

Box, G.E.P., & Cox, D.R. (1964, July). An analysis of transformations. *J. R. Stat. Soc. Series B Stat. Methodol.*, 26(2), 211–252, <https://doi.org/10.1111/J.2517-6161.1964.TB00553.X>

Cramér, H. (1928, January). On the composition of elementary errors. *Scand. Actuar. J.*, 1928(1), 13–74, <https://doi.org/10.1080/03461238.1928.10416862>

Croux, C., & Rousseeuw, P.J. (1992, January). A class of high-breakdown scale estimators based on subranges. *Commun. Stat. Theory Methods*, 21(7), 1935–1951, <https://doi.org/10.1080/03610929208830889>

D'Agostino, R.B., & Belanger, A. (1990). A suggestion for using powerful and informative tests of normality. *Am. Stat.*, 44(4), 316–321, <https://doi.org/10.2307/2684359>

De Cock, D. (2011, November). Ames, iowa: Alternative to the boston housing data as an end of semester regression project. *J. Stat. Educ.*, 19(3), , <https://doi.org/10.1080/10691898.2011.11889627>

Gijbels, I., Karim, R., Verhasselt, A. (2019). Quantile estimation in a generalized asymmetric distributional setting. *Stochastic models, statistics and their applications* (pp. 13–40). Springer International Publishing.

Gorman, K.B., Williams, T.D., Fraser, W.R. (2014, March). Ecological sexual dimorphism and environmental variability within a community of antarctic penguins (genus pygoscelis). *PLoS One*, 9(3), e90081, <https://doi.org/10.1371/journal.pone.0090081>

Griffin, M. (2018, January). *gnorm: Generalized normal/exponential power distribution*. The R Foundation.

Huber, P.J. (1981). *Robust statistics*. John Wiley & Sons.

Jarque, C.M., & Bera, A.K. (1980, January). Efficient tests for normality, homoscedasticity and serial independence of regression residuals. *Econ. Lett.*, 6(3), 255–259, [https://doi.org/10.1016/0165-1765\(80\)90024-5](https://doi.org/10.1016/0165-1765(80)90024-5)

- Kuhn, M., & Johnson, K. (2019). *Feature engineering and selection: A practical approach for predictive models*. Chapman and Hall/CRC.
- Loprinzi, C.L., Laurie, J.A., Wieand, H.S., Krook, J.E., Novotny, P.J., Kugler, J.W., ... Klatt, N.E. (1994, March). Prospective evaluation of prognostic variables from patient-completed questionnaires. north central cancer treatment group. *J. Clin. Oncol.*, 12(3), 601–607, <https://doi.org/10.1200/JCO.1994.12.3.601>
- Nadarajah, S. (2005, September). A generalized normal distribution. *J. Appl. Stat.*, 32(7), 685–694, <https://doi.org/10.1080/02664760500079464>
- Powell, M.J.D. (2009). *The BOBYQA algorithm for bound constrained optimization without derivatives* (Tech. Rep. No. Cambridge NA Report NA2009/06). University of Cambridge.
- Raymaekers, J., & Rousseeuw, P.J. (2024, August). Transforming variables to central normality. *Mach. Learn.*, 113(8), 4953–4975, <https://doi.org/10.1007/s10994-021-05960-5>
- Romano, J.D., Le, T.T., La Cava, W., Gregg, J.T., Goldberg, D.J., Chakraborty, P., ... Moore, J.H. (2022, January). PMLB v1.0: an open-source dataset collection for benchmarking machine learning methods. *Bioinformatics*, 38(3), 878–880, <https://doi.org/10.1093/bioinformatics/btab727>
- Rousseeuw, P.J., & Croux, C. (1993, December). Alternatives to the median absolute deviation. *J. Am. Stat. Assoc.*, 88(424), 1273, <https://doi.org/10.2307/2291267>
- Shapiro, S.S., & Wilk, M.B. (1965). An analysis of variance test for normality (complete samples). *Biometrika*, 52(3/4), 591–611, <https://doi.org/10.2307/2333709>
- Subbotin, M.T. (1923). On the law of frequency of error. *Mat. Sb.*, 31(2), 296–301,
- Tukey, J.W. (1957, September). On the comparative anatomy of transformations. *Ann. Math. Stat.*, 28(3), 602–632, <https://doi.org/10.1214/AOMS/1177706875>
- Tukey, J.W. (1967). An introduction to the calculations of numerical spectrum analysis. B. Harris (Ed.), *Advanced seminar on spectral analysis of time series*. New

York: John Wiley and Sons, Inc.

Tukey, J.W. (1977). *Exploratory data analysis*. Addison-Wesley Publishing Company.

von Mises, R. (1928). *Wahrscheinlichkeit statistik und wahrheit*. Springer-Verlag Berlin, Heidelberg.

Wright, M.N., & Ziegler, A. (2017). ranger: A fast implementation of random forests for high dimensional data in C++ and R. *Journal of Statistical Software*, 77(1), 1–17, <https://doi.org/10.18637/jss.v077.i01>

Yeo, I., & Johnson, R.A. (2000, December). A new family of power transformations to improve normality or symmetry. *Biometrika*, 87(4), 954–959, <https://doi.org/10.1093/biomet/87.4.954>

Zwanenburg, A., & Löck, S. (2025a). *familiar: End-to-end automated machine learning and model evaluation*. Retrieved from <https://github.com/oncoray/familiar>

Zwanenburg, A., & Löck, S. (2025b). *power.transform: Location and scale invariant power transformations*. Retrieved from <https://github.com/oncoray/power.transform>